Compound soil and atmospheric drought events and CO_2 fluxes of a mixed deciduous forest: Occurrence, impact, and temporal contribution of main drivers

Liliana Scapucci[1,*,♦], Ankit Shekhar[1,♦], Sergio Aranda-Barranco[2], Anastasiia Bolshakova[3], Lukas Hörtnagl[1], Mana Gharun[4], Nina Buchmann[1]

[1] Department of Environmental Systems Science, ETH Zürich, Switzerland
[2] Department of Ecology, University of Granada, Granada, Spain
[3] University of Natural Resources and Life Sciences, Vienna (BOKU), Austria
[4] Department of Geosciences, University of Münster, Germany

**Correspondence to*: Liliana Scapucci (liliana.scapucci@usys.ethz.ch)

♦Both the authors contributed equally to the manuscript

Abstract. With global warming, forests are facing an increased exposure to compound soil and atmospheric drought (CSAD) events, characterized by low soil water content (SWC) and high vapor pressure deficit (VPD). Such CSAD events trigger responses in both ecosystem and forest floor CO_2 fluxes, of which we know little about. In this study, we used multi-year daily and daytime above-canopy (18 years; 2005-2022) and daily forest floor (five years; 2018-2022) eddy-covariance CO_2 fluxes of a Swiss forest site (montane mixed deciduous forest; CH-Lae). The objectives were (1) to characterize CSAD events at CH-Lae; (2) to quantify the impact of CSAD events on ecosystem and forest floor daily CO_2 fluxes; and (3) to identify the major drivers and their temporal contributions to changing ecosystem and forest floor CO_2 fluxes during CSAD events and CSAD growing seasons. Our results showed that the growing seasons of 2015, 2018, and 2022 were the top three driest at CH-Lae since 2005 (referred to as CSAD years), with similar intensity and duration of the respective CSAD events, but with considerably different pre-drought conditions. The CSAD events reduced daily mean net ecosystem productivity (NEP) in all three CSAD years by about 38% compared to the long-term mean, with the highest reduction during 2022 (41%). This reduction in daily mean NEP was largely due to decreased gross primary productivity (GPP; >16% compared to the long-term mean) rather than increased ecosystem respiration (Reco) during CSAD events. Furthermore, forest floor respiration (Rff) decreased during the CSAD events in 2018 and 2022 (no measurements in 2015), with a larger reduction in 2022 (41%) than in 2018 (16%) compared to the long-term mean (2019-2021). Using data-driven machine learning methods, we identified the major drivers of NEP and Rff during CSAD events. While daytime mean NEP (NEP_{DT}) during 2015 and 2018 CSAD events was limited by VPD or SWC, respectively, NEP_{DT} during the 2022 CSAD event was strongly limited by both SWC and VPD. Air temperature had negative effects, while net radiation showed positive effects on NEP_{DT} during all CSAD events. Daily mean Rff during the 2018 CSAD event was driven by soil temperature and SWC, but severely limited by SWC during the 2022 CSAD event. We found that a multi-layer analysis of CO_2 fluxes in forests is necessary to better understand forest

responses to CSAD events, particularly if the first signs of NEP acclimation to CSAD events - we saw for our forest - are found elsewhere as well. We conclude that CSAD events have multiple drivers with different temporal contributions, making predictions of site-specific CSADs and forest long-term responses to such conditions more challenging.

1 Introduction

Forests play an essential role in mitigating climate change thanks to their ability to partially offset anthropogenic CO_2 emissions (Harris et al., 2021). However, the increasing frequency of droughts and heatwaves is compromising the carbon uptake capacity of forests worldwide (Anderegg et al., 2022). According to IPCC (2022), the temperature increase over Europe (1850-1990) has been about twice the global mean since the pre-industrial period, accompanied with an increase in frequency of drought events (Spinoni et al., 2018). Recent studies have revealed that European forests are showing increasing rates of tree mortality, induced by low soil water content (SWC) (George et al., 2022). In addition, recent studies have highlighted the role of high vapor pressure deficit (VPD), an indicator of atmospheric drought and a distinct characteristic of heatwaves, further exacerbating tree mortality (Birami et al., 2018; Gazol and Camarero, 2022; Grossiord et al., 2017, 2020). Due to enhanced land-atmosphere feedback in response to climate change, the frequency of co-occurring low soil moisture and high VPD conditions has also increased (Dirmeyer et al., 2021; Miralles et al., 2019; Orth 2021; Zhou et al., 2019), resulting in so-called compound soil and atmospheric drought (CSAD) conditions. The 21st century European droughts in 2003, 2015, 2018, and the most recent one in 2022, were indeed characterized by CSAD conditions (Dirmeyer et al., 2021; Ionita et al., 2021, 2017; Lu et al., 2023; Tripathy and Mishra, 2023). In 2022, Europe experienced its hottest and driest year on record, with the summer being the warmest ever recorded, which ultimately led to numerous CSAD events across the continent (Copernicus Climate Change Service, 2023).

Such CSAD events have multiple impacts on forest ecosystems. They can lead to reduced net ecosystem productivity (NEP) by decreasing gross primary productivity (GPP) and/or increasing ecosystem respiration (Reco) (Xu et al., 2020). Additionally, soil respiration (SR) can be reduced due to water scarcity in the soil, which limits both heterotrophic and autotrophic respiration (Ruehr and Buchmann, 2009; Ruehr et al., 2010; van Straaten et al., 2011; Sun et al., 2019; Schindlbacher et al., 2012). However, high soil temperature (TS) can increase SR rates when soil moisture is not limiting metabolic reactions in the soil (Schindlbacher et al., 2012), affecting the sensitivity of respiration to soil temperature (Sun et al., 2019). Thus, to better understand the ecological consequences of climate change on forest ecosystems, the capacity of forests to acclimate to stress conditions like CSAD events, e.g., by changing the NEP sensitivity to abiotic drivers like air temperature (Tair), VPD, and SWC during a growing season or among growing seasons, needs to be known (Grossman, 2023).

The summer of 2022 in Europe, characterized by strong CSAD conditions (Tripathy and Mishra, 2023; van der Woude et al., 2023), showed an extensive reduction in forest greenness (about 30% of temperate and Mediterranean European forest area; Hermann et al., 2023), and a reduction in GPP (van der Woude et al., 2023), comparable to summer 2018 CSAD events. In 2018, this resulted in drought-induced tree mortality in Scots pine (*Pinus sylvestris* L.) and European beech (*Fagus sylvatica*

L.) forests (Haberstroh et al., 2022; Obladen et al., 2021; Rukh et al., 2023; Schuldt et al., 2020). Clearly, most drought impact studies use data measured above the canopy, i.e., net carbon dioxide (CO_2) exchange or remote sensing of vegetation. Particularly the latter is largely neglecting the below-canopy component of the forest (also known as forest floor), although it might show contrasting responses to drought conditions compared to the top canopy sensed from above (Chi et al., 2021). The forest floor, composed of soil, tree roots, woody debris, and understory vegetation, provides an essential interface for soil-atmosphere CO_2 exchange, with photosynthesis of understory vegetation and forest floor respiration (Rff), both representing major CO_2 exchange processes (Chi et al., 2017; Paul-Limoges et al., 2017). Therefore, separating the ecosystem-level drought response from the forest floor drought response provides a more comprehensive insight into drought impacts than one level alone (Chi et al., 2017; Martinez-Garcia et al., 2022). Furthermore, the intensity and duration of CSAD events, and their impacts on forests can largely vary at regional scale (Pei et al., 2013; Kim et al., 2020). Thus, more attention is needed on temperate forest ecosystems across Central Europe, such as in Switzerland, where forests are accustomed to humid and cool climates, with ample amount of summer rainfalls (Schuldt and Ruehr, 2022).

In Switzerland, 2022 was the warmest year on record since the beginning of instrumental measurements in 1864, with average air temperatures 1.6 °C above the long-term mean (1991-2020), and annual precipitation amounting to only 60% of the long-term average (MeteoSvizzera, 2023). Such hot and dry conditions as in 2022 were bound to result in CSAD events which could ultimately compromise the CO_2 uptake capacity of forests. Thus, the objectives of this study were as follows: (1) to characterize compound soil and atmospheric drought (CSAD) events at a Swiss montane mixed deciduous forest site, (2) to quantify the impact of CSAD events on ecosystem and forest floor CO_2 fluxes, and (3) to identify the major drivers of ecosystem and forest floor CO_2 fluxes and their temporal contributions during CSAD events and CSAD growing seasons.

2 Material and methods

2.1 Forest site

The study was conducted in a managed mixed deciduous mountain forest (CH-Lae at 682 m a.s.l.) located at the Lägeren, in the far east of the Jura Mountain range in Switzerland. The CH-Lae forest has a complex canopy structure with a rather high species diversity, the dominant species are European beech (*Fagus sylvatica* L., 40% cover), ash (*Fraxinus excelsior* L., 19% cover), Sycamore maple (*Acer pseudoplatanus* L., 13% cover), European silver fir (*Abies alba* Mill., 8% cover), large-leaved linden (*Tilia platyphyllos* Scop., 8%) and Norway spruce (*Picea abies* (L.) H. Karst., 4% cover) (Paul-Limoges et al., 2020), showing no significant trend of leaf area index (LAI) over the years. The soils at CH-Lae are characterized by two main types, rendzic leptosols and haplic cambiosols, with bedrocks of limestone marl, sandstone, and transition zones between the two (Ruehr et al., 2010). The mean annual air temperature at CH-Lae was 8.8 ± 1.3 °C (mean ± SD), and mean annual precipitation was 831 ± 121 mm (mean 2005-2022). The understory vegetation at CH-Lae is dominated by wild garlic (*Allium ursinum* L., height ~ 30 cm) which grows for a short period in spring and early summer (March-June) (Ruehr and Buchmann, 2009). The net carbon uptake period of CH-Lae is from May to September (Figure A1).

2.2 Ecosystem-level measurements

In this study, we used measurements of ecosystem CO_2 fluxes from above the forest canopy using the eddy covariance (EC) technique (Aubinet et al., 2012), spanning from 2005-2022. The EC system (eddy tower coordinates: 47°28'42.0" N and 8°21'51.8" E) was mounted at a height of 47 m (mean canopy height of 30 m) above the ground. The EC technique utilizes high frequency (20 Hz) measurements of wind speed and wind direction, measured with a three-dimensional sonic anemometer, and gas (here CO_2) concentration, measured with an infrared gas analyser (IRGA) as CO_2 molar density (with an open-path IRGA from 2004-2015) or as dry mole fraction (with a closed-path IRGA from 2016-2022; for details of instrumentation used in the EC system, see Table A1). The time-lag between turbulent fluctuations of vertical wind speed and CO_2 molar density or dry mole fraction was calculated by covariance maximization (Fan et al., 1990); half-hourly fluxes of CO_2 (FC, µmol CO_2 m^{-2} s^{-1}) were then calculated from the 20 Hz measurements using the EddyPro software v7 (v7.0.9, LI-COR Inc., Lincoln, NE, USA), following established community guidelines (Aubinet et al., 2012; Sabbatini et al., 2018). The FC from the open-path IRGA LI-7500 were corrected for air density fluctuations (Webb et al., 1980), all FC underwent spectral corrections for high-pass (Moncrieff et al., 2004) and low-pass filtering (Fratini et al., 2012; Horst, 1997) losses. The impact of self-heating of the open-path IRGA on FC was corrected based on a method described by Kittler et al. (2017). The net ecosystem CO_2 exchange (NEE) was calculated as the sum of FC and the CO_2 storage term estimated from concentrations based on 1-point measurements (Greco and Baldocchi, 1996). The quality of half-hourly NEE flux values was ensured by applying a comprehensive quality screening process that combined several well-tested methods into a single quality flag (0-1-2 system; Mauder and Foken, 2006; Sabbatini et al., 2018). Fluxes of low quality (flag = 2) were removed from further analyses. Fluxes that passed the quality-screening process were then gap-filled (Reichstein et al., 2005) and partitioned into gross primary productivity (GPP) and ecosystem respiration (Reco) using the day-time partitioning method (Lasslop et al., 2010). More details about quality-screening, gap-filling and partitioning can be found in Shekhar et al. (2024). In this study, we used net ecosystem productivity (NEP = –NEE) for further data analyses. Positive NEP fluxes represent CO_2 uptake by the forest, whereas negative NEP represents CO_2 release. Along with fluxes, we also measured half-hourly Tair, relative humidity (RH), incoming short-wave radiation (Rg), and precipitation (Precip) at the top of the EC tower from 2005-2022 (see Table A1 for instrumentation details). We estimated half-hourly VPD from half-hourly measurements of air temperature and relative humidity.

2.3 Forest floor measurements

We measured forest floor fluxes of CO_2 based on the EC technique (Aubinet et al., 2012) below the canopy from 2018 to 2022 to estimate net ecosystem exchange of the forest floor (NEE_{ff}), which includes CO_2 fluxes from the soil and the understory vegetation. We partitioned NEE_{ff} into gross primary productivity of the forest floor (GPP_{ff}) and respiration of the forest floor (Rff; Lasslop et al., 2010). The below-canopy station at CH-Lae site was located in a distance of c. 100 m from the main tower (47°28'42.9" N and 8°21'27.6" E) and had a height of 1.5 m. Wind speed and direction were measured with a sonic anemometer and CO_2 concentrations with an open-path IRGA (LI-7500; Table A1) at a frequency of 20 Hz. We calculated NEE_{ff}, and the partitioned fluxes, using the same process and corrections as for above-canopy measurements (except for the self-heating correction). We used a seasonal u* filtering to account for changes in the understory canopy, with 0.024 ms^{-1} for spring (day 60-151), 0.027 ms^{-1} for summer (day 152-243), 0.039 ms^{-1} for autumn (day 244-334), and 0.025 ms^{-1} for winter (day 335-60). Additionally, we continuously measured air temperature ($Tair_{ff}$), relative humidity (RH_{ff}), incoming short-wave radiation (Rg_{ff}), soil temperature (TS) and soil water content (SWC) at 5, 10, 20, 30, 50 cm depth at the forest floor meteorological station next to the below-canopy EC system (Table A1). In 2020, we installed an additional soil moisture profile. To account for spatial heterogeneity, we normalized the SWC data using a z-score transformation, we then used z-scores of SWC for further analyses.

2.4 Soil respiration measurements

Ten PVC collars (diameter 20 cm, height 13 cm, depth = 2 cm) were installed at CH-Lae in spring 2022, at the same locations within the footprint of the tower as described in Ruehr et al. (2010). Soil respiration (SR) measurement campaigns were performed at least once a month from March until November 2022, with a LI-8100-103 analyser and a closed chamber (Table A1). Collars were measured once a day in a random order during each campaign. Every measurement lasted 90 seconds from the moment the LI-8100 chamber closed on top of the collar. Next to each collar, we measured SWC_S (SWC from survey measurements) at 5 cm with a soil moisture sensor, and TS_S (TS from survey measurements) at 5 cm with a temperature sensor (Table A1). When the Swiss meteorological service (MeteoSwiss) forecasted a two-week heatwave starting on 14th of July 2022, we intensified the measurements of SR to one campaign every second day with two rounds of measurements per day for two weeks (at 09:00 and at 16:00). The order of measurements was inverted every fieldwork day. Since the portable soil moisture sensor broke on 22nd of July 2022 and was only available on 11th of August 2022, we calculated the SWC based on continuous measurements at the forest floor meteorological station for these days ($SWCs = 1.34 * SWC - 10.7$; $R^2 = 0.82$).

2.5 Data analyses

In this study, we focused all our analyses on the growing season, between May and September, when the long-term mean of ecosystem NEP (2005-2022) was positive, implying that GPP of the vegetation overcompensated all respiratory losses (Figure A1; Körner et al., 2023). We conducted all data analyses using the R programming language (R version 4.3.3, R core team, 2021). We compared cumulative precipitation (indicating total water supply to the forest) and cumulative VPD (indicating total atmospheric water demand) during the growing seasons of 18 years at our forest site and chose the three years with the driest growing seasons, i.e., with low cumulative precipitation and high VPD, called compound soil and atmospheric drought (CSAD) years hereafter. Then, we identified the CSAD events during these CSAD years as periods when both soil and atmosphere were significantly drier than usual for more than 10 consecutive days, implying a compound drought condition. To identify drier than usual periods, we compared 5-day moving daily means (assigned to the centre of 5 days) of SWC and

VPD with their long-term (2005-2022) means. So, a period of 10 or more consecutive days with SWC being significantly lower ($p<0.05$) and VPD being significantly higher ($p<0.05$) than the long-term mean, was identified as CSAD event.

We quantified the impact of CSAD events based on anomalies of NEP, GPP, Reco, and Rff by comparing them with their respective long-term means (NEP, GPP, Reco: mean of 2005-2022; Rff: mean of 2019-2021). Since CSAD events occurred in two of the five years of flux data available at the forest floor station (Rff), we excluded 2018 and 2022 from the calculation of the Rff long-term mean. To understand the major drivers of NEP and Rff, we performed two different driver analyses in this study, first focusing on the CSAD years (I), and second focusing on the CSAD events in the CSAD years (II).

(I) For the first driver analysis, we used the conditional variable importance (CVI) feature based on random forest regression model (Breiman, 2001). For modelling daily mean NEP (NEP), the predictors were Rg, VPD, and Tair measured above the canopy, and SWC measured at the forest floor station, whereas for modelling daily mean Rff (Rff), the predictors were Rg (Rg_{ff}) and Tair ($Tair_{ff}$) as well as soil temperature (TS) and SWC, measured at the forest floor station. The model was run for each year separately. The CVI is specifically designed to consider the multi-collinearity among predictors (i.e., Tair, VPD, Rg), while estimating the importance of each predictor variable (Strobl, et al., 2008), and thus considered a very reliable method to estimate overall feature importance. For estimating CVI, we used the *cforest* and *varimp* function from the R-package *party* (Hothorn et al., 2006).

(II) For the second driver analysis, we used daytime mean NEP (NEP_{DT}, excluding nighttime data to highlight the effects of environmental drivers when photosynthesis is dominating) to avoid potential biases if GPP were used, since some predictors (i.e., Tair and Rg) were used to partition NEE into GPP and Reco. We used a TreeExplainer-based SHapley Additive exPlanations (SHAP) framework (Lundberg and Lee, 2017; Lundberg et al., 2020), with a tree-based ensemble learning extreme gradient boosting (XGB) model (Chen and Guestrin, 2016). The XGB model was used to model NEP_{DT} and Rff, applying the GridSearchCV methodology to optimize the parameters of the XGB model for NEP and Rff (see Wang et al., 2022 for more details). The TreeExplainer-based SHAP framework integrates explanatory models (here the XGM model) with game theory (Shapley, 1953), which allowed us to estimate the marginal contribution (known as SHAP value) of each predictor variable (i.e., Tair, VPD, SWC, TS) to the response variables (NEP_{DT}, Rff). We used the function *xgboost* (eXtreme Boosting Training) from the R-package *xgboost* to train the model, and the functions *shap.values* and *shap.prep* from the R-package *SHAPforxgboost* (Chen and Guestrin, 2016) to obtain the SHAP values of each predictor variable for NEP_{DT} (for 2005-2022) and Rff (for 2018-2022). The models were run for each year separately, and we obtained the marginal contributions of each feature for each day of each growing season, which allowed to observe their temporal course. Then we calculated the mean SHAP value during the CSAD events for each predictor of NEP_{DT} and Rff for the CSAD years to determine the dominant direction of the effect of each feature. To determine differences to the long-term means, we also calculated the mean SHAP values of the predictors during the respective reference periods (long-term means: 2005-2022 for NEP_{DT}; 2019-2021 for daily Rff). The respective reference period included all days, in which a CSAD event occurred independent of the year, i.e., ranging from 7th July to 23rd August for NEP_{DT} during 2005-2022 (including CSAD years due to the large number of years available with measurements), and from 14th July to 23rd August for Rff during 2019-2021 (excluding CSAD years due to the small number of years available with measurements; Figure A2). For comparison with the first model (based on CVI), we also calculated the mean and standard error of the absolute SHAP values for NEP in 2015, 2018, 2022, and the long-term mean 2005-2022 (Figure A3). However, since we were interested in the short-term changes in driver importance, including the direction of their effect, we did not follow up using absolute SHAP values in this study.

We then used the SHAP values of drivers (VPD, Tair and SWC for NEP_{DT}; TS and SWC for Rff) to estimate acclimation of NEP_{DT} and Rff to abiotic drivers by estimating the absolute driver values (thresholds) related to the largest effects, as indicated by the maximum marginal contributions to the response variables NEP_{DT} and Rff for each CSAD year (Gou et al., 2023; Wang et al., 2022). For this, we fitted a local polynomial regression between the SHAP values of the driver variable and the driver variable itself, i.e., a loess curve, and calculated the residual standard error from the loess function of the *stats* R-package. We then identified the absolute driver value corresponding to the highest SHAP value (feature_NEPmax, feature_Rffmax) for each CSAD year, i.e., VPD_NEP_{max}, $Tair\_NEP_{max}$, SWC_NEP_{max}, the VPD, Tair and SWC values associated with the highest marginal contributions to NEP_{DT}, as well as TS_Rff_{max} and SWC_Rff_{max}, i.e., TS and SWC values associated with the highest marginal contributions to Rff. These absolute driver values provided information about the NEP_{DT} and Rff sensitivities to abiotic drivers during the growing season of each CSAD year. For example, a shift in the SWC_NEP_{max} towards drier conditions in one growing season compared to others thus translated to an acclimation of NEP_{DT} to drier conditions in that growing season. To test if the feature_NEPmax values varied with the corresponding mean feature values during the respective growing season, we fitted a linear regression between the mean VPD, SWC and Tair and their corresponding values of NEPmax for each year from 2005 to 2022.

Finally, we used linear models to explain daily mean SR responses to TS and SWC during the CSAD events and the rest of the years, based on the measurements from the survey campaigns in 2022. The amount of SR data was not sufficient to use machine learning approaches.

3 Results

3.1 Detected CSAD events

The growing seasons (May to September) of 2015, 2018, and 2022 were the three driest in the last 18 years (2005-2022) which the mountain forest site experienced (Figure 1). The growing seasons in these three years were characterized by very high atmospheric drought (indicated by cumulative VPD) and low water supply (indicated by cumulative precipitation, a proxy for soil drought) In particular, the summer months (June-August) of these three years were significantly warmer and drier (Figures 1, 2). Mean summer temperatures of 2018 (19.8 °C) and 2022 (20.3 °C) were more than 2.5 °C higher than the long-term mean summer temperature at the forest site (17.2 °C); summer precipitation sums in 2018 and 2022 were more than 20% and 10% lower than the long-term mean cumulative summer precipitation (300 mm), respectively. Furthermore, during the month July of both years 2015 and 2022, less than one-third of long-term mean cumulative summer precipitation was recorded. Coupled with a more than 50% increase in average VPD, this resulted in intense soil and atmospheric drought conditions.

Moreover, we detected two distinct CSAD events in 2015, i.e., periods of 10 or more consecutive days with significantly lower SWC and significantly higher VPD than the long-term mean: one from 7th July 2015 to 21st July 2015, and a second one from 2nd August 2015 to 13th August 2015 (Figure 2a, d, g), comprising a total of 27 days with a mean maximum temperature of 26.9 °C, mean maximum VPD of 2.24 kPa, and mean minimum normalized SWC of -1.83 (Table 1). For comparison, in 2018, the CSAD event lasted for 32 days, from 23rd July 2018 to 23rd August 2018 (Figure 2b, e, h), with a mean maximum temperature of 27.7 °C, mean maximum VPD of 2.19 kPa, and mean minimum normalized SWC of -1.94 (Table 1). In 2022, the CSAD event lasted 22 days, from 14th July 2022 to 4th August 2022. Thus, although it was shorter than in those in 2015 and 2018 (Figure 2c, f, i), it was more intense than those in 2015 and 2018, with mean maximum temperature of 28.3 °C, mean minimum VPD of 2.43 kPa, and mean minimum normalized SWC of -2.51 (Table 1). We measured the highest air temperature (33.56 °C) and the third highest VPD (3.83 kPa) ever recorded at the forest site in the past 18 years (2005-2022) on the last day of the 2022 CSAD event, i.e., on 4th August 2022 between 16:30 and 17:00 (Figure A4). Furthermore, the 2022 CSAD event was characterized by multiple tropical nights (i.e., nighttime temperature > 20 °C; Figure A4) and progressive soil drying (Figure 2).

Thus, the CSAD events were not only slightly different in terms of intensities, but also in terms of time of CSAD occurrence (Table 1), and initial drought development. In both years 2015 and 2018, wetter (than long-term mean; 2015) or normal (2018) soil conditions continued from late spring (mid-May) until end of June, with a quick soil drought intensification in July due to high air temperatures (> 30°C), high VPD (>3.8 kPa) (Figure 2), and low precipitation (more than 40% lower than the long-term July average). The year 2022, however, was already characterized by exceptionally low soil water content and high VPD (> 2.5 kPa) in May (Figure 2i), which intensified with low precipitation and high temperatures into early summer. Nighttime VPD exceeded 2 kPa on a few days in June, before the CSAD event occurred mid-July to beginning of August (see Figure A4). Even the heavy rainfall on 5th August 2022 (28 mm) only resulted in a minor increase of SWC. Nevertheless, after 4th August, air temperature and VPD conditions became near-normal, thereby marking the end of the 2022 CSAD event (Figure 2).

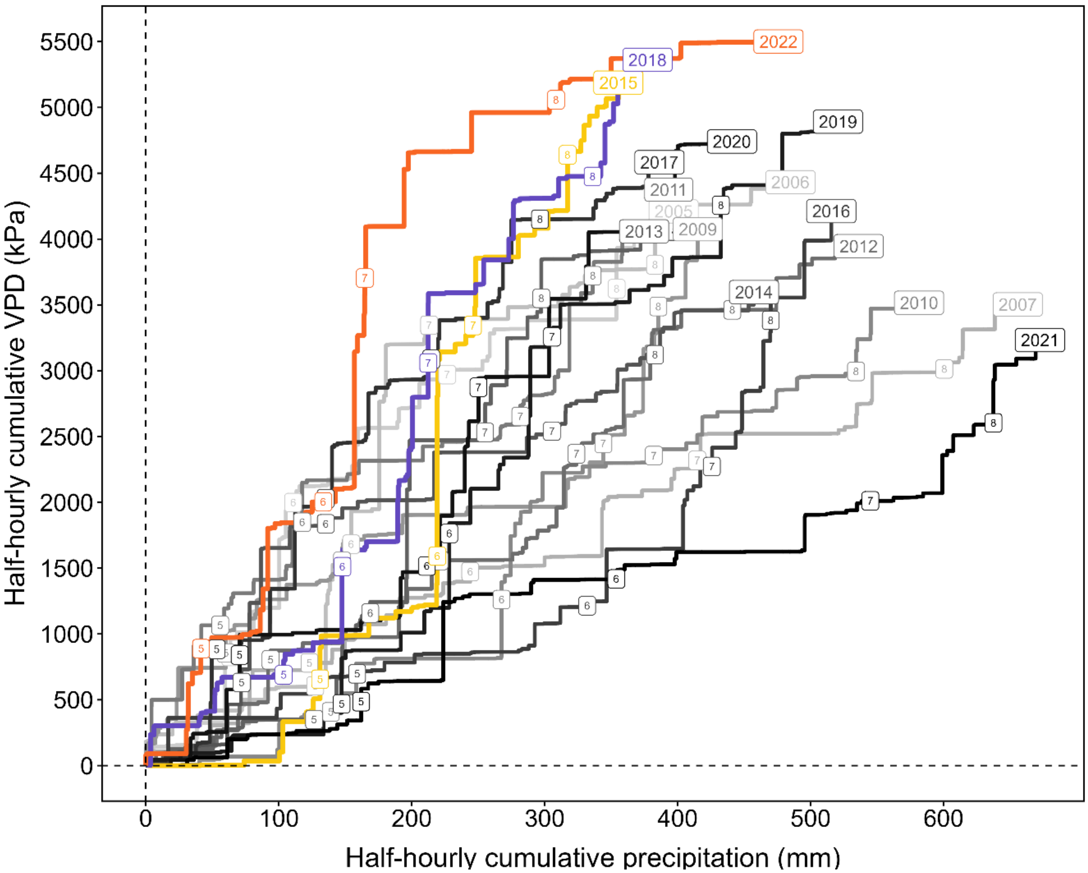

Figure 1. Cumulative VPD and cumulative precipitation from May to September (growing season of the Lägeren forest) of each year (2005-2022). The numbers (5-9) on the cumulative lines depict the end of each month.

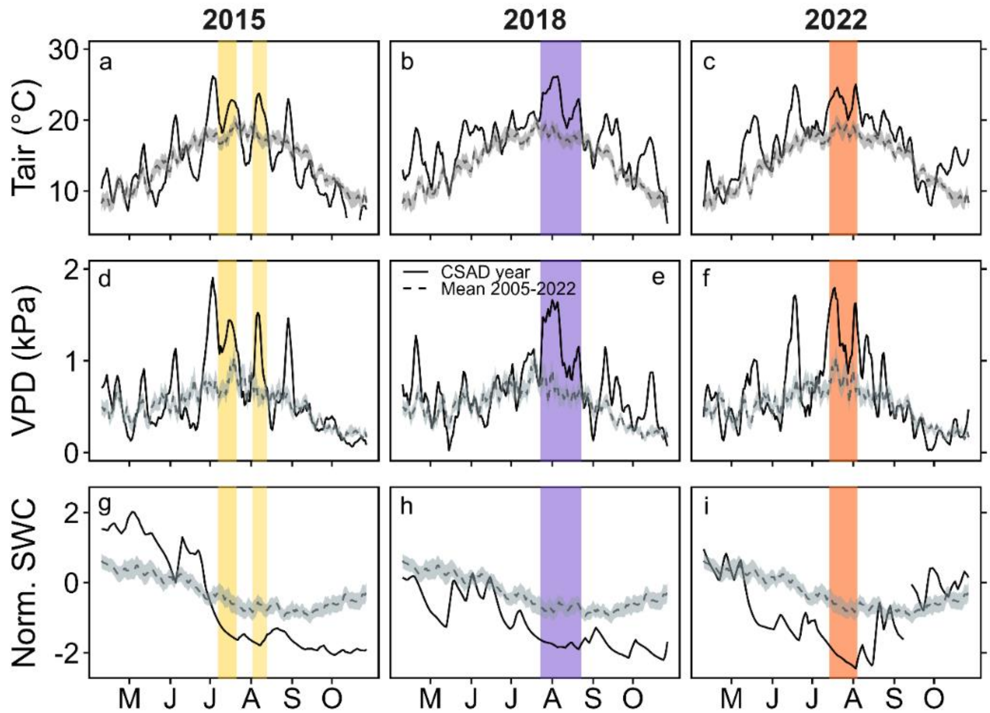

Figure 2. Comparison of 5 day moving averages of daily mean (a-c) Tair, (d-f) VPD, and (g-i) SWC in the years when a CSAD event happened against the long-term means (2005-2022). The band around the dashed line indicates the standard error of the long-term mean 2005-2022. The coloured areas mark the CSAD events, i.e., periods with co-occurring lowest SWC and highest VPD.

Table 1. Characterization of CSAD events in 2015, 2018 and 2022. Duration, maximum (Max.) and standard deviation (± SD) of daily mean Tair, maximum (Max.) and standard deviation (± SD) of daily mean VPD, and minimum (Min.) and standard deviation (± SD) of daily mean normalized SWC recorded during the CSAD events in 2015, 2018 and 2022 are given.

Year	Duration (days)	Max. ± SD Tair (°C)	Max. ± SD VPD (kPa)	Min. ± SD SWC (normalized)
2015	15 + 12 = 27	26.9 ± 3.03	2.24 ± 0.4	-1.83 ± 0.20
2018	32	27.7 ± 2.88	2.19 ± 0.5	-1.93 ± 0.10
2022	22	28.3 ± 2.64	2.43 ± 0.5	-2.51 ± 0.20

3.2 Impacts of CSAD events on CO_2 fluxes

All CSAD events had immediate negative impacts on ecosystem CO_2 fluxes, showing a decrease in the CO_2 fluxes compared to the long-term means (Table 2, Figure 3a, c, e, g). Mean daily NEP, GPP, Reco and Rff tended to be lower during the CSAD events compared to the respective long-term means of the reference periods 2005-2022 (for NEP, GPP and Reco) and 2019-2021 (for Rff; Table 2), with much larger variations during CSAD events compared to those of the reference periods (except for Rff; Figure 3b, d, f, h). The lowest average NEP was recorded in the CSAD event of 2022 (minus 41%), followed by NEP in the 2018 and 2015 CSAD events (minus 38% and minus 35%, respectively), while the lowest average GPP and Reco were found in the 2018 CSAD event (minus 28% and minus 31%, respectively; Table 2).

All cumulative CO_2 fluxes decreased during CSAD events in 2015, 2018 and 2022 compared to the long-term means (Figure 3b, d, f, h), with the only exception of Reco in 2022. The cumulative NEP during the CSAD events in 2015 and 2018 decreased by 34 µmol CO_2 m^{-2} s^{-1} and 26 µmol CO_2 m^{-2} s^{-1}, respectively, compared to the respective long-term mean of the reference period (2005-2022; Figure 3b). During both CSAD years 2015 and 2018, cumulative GPP and Reco decreased considerably, although cumulative GPP tended to decrease more (>40 µmol CO_2 m^{-2} s^{-1}) than Reco (>30 µmol CO_2 m^{-2} s^{-1}; Figure 3d, f). In contrast, during the CSAD event in 2022, cumulative NEP decreased by 27 µmol CO_2 m^{-2} s^{-1} compared to long-term mean (Figure 3b), due to a decrease in cumulative GPP (by 44 µmol CO_2 m^{-2} s^{-1}) and only negligible changes in Reco (Figure 3d, f). Furthermore, Rff fluxes during the 2018 and 2022 CSAD events were lower compared to the long-term mean of the reference period (2019-2021), with 23 µmol CO_2 m^{-2} s^{-1} and 32 µmol CO_2 m^{-2} s^{-1}, respectively (Figure 3h). This decrease in Rff was supported by decreasing daily mean SR rates measured in 2022 (Figure 3g).

Table 2. Daily mean CO_2 fluxes during CSAD events in 2015, 2018 and 2022 as well as their long-term means during the respective reference periods. Means and standard deviation (± SD) of net ecosystem production (NEP), partitioned gross primary productivity (GPP) and ecosystem respiration (Reco) as well as forest floor respiration (Rff) are given. The reference period for NEP, GPP and Reco represents all days between the 7th of July and the 23rd of August during 2005 and 2022; the reference period for Rff represents all days between the 14th of July and 23rd of August during 2019 and 2021. All fluxes are given in µmol CO_2 m^{-2} s^{-1}. n.a. = not available.

	NEP	GPP	Reco	Rff
CSAD 2015	2.09 ± 2.14	7.33 ± 2.54	5.05 ± 2.11	n.a.
CSAD 2018	1.99 ± 1.36	6.31 ± 1.44	4.23 ± 0.89	3.19 ± 0.68
CSAD 2022	1.89 ± 1.77	6.69 ± 1.33	5.73 ± 1.55	2.24 ± 0.20
Reference period	3.2 ± 0.82	8.77 ± 0.85	6.14 ± 0.65	3.81 ± 0.26

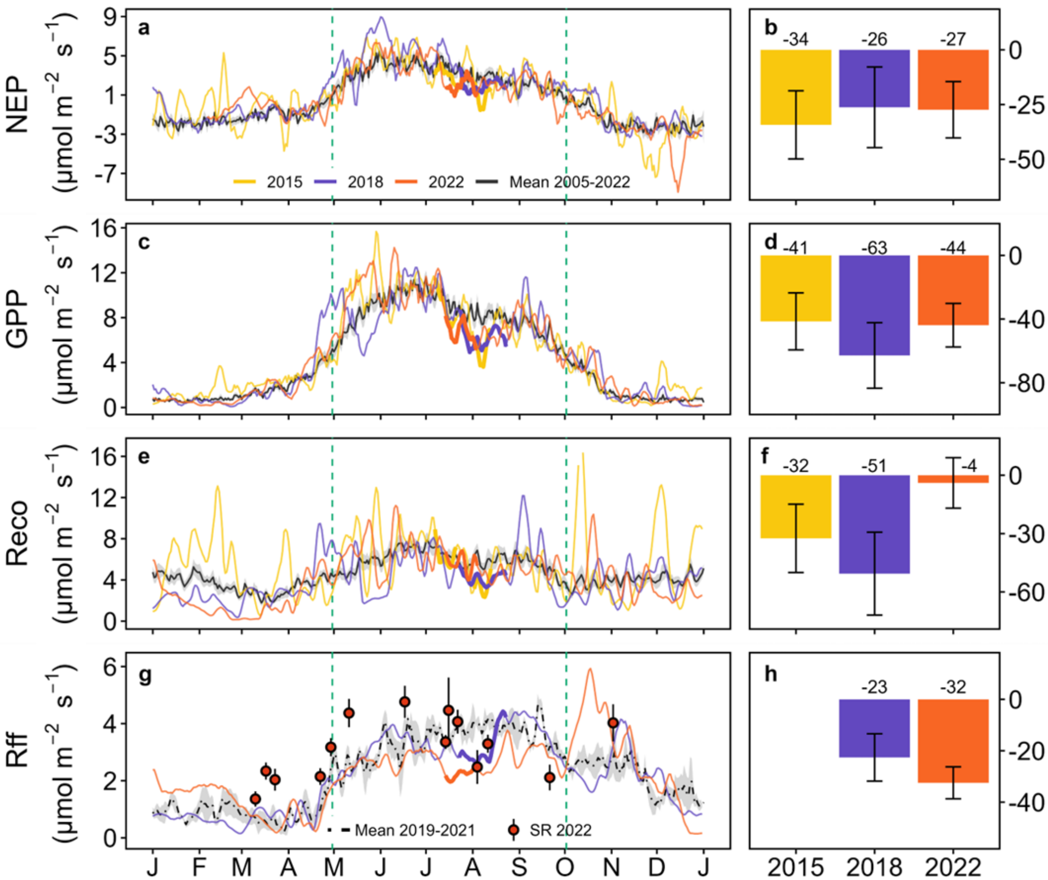

Figure 3. Comparison of daily mean (a) net ecosystem production (NEP), (c) gross primary productivity (GPP), (e) ecosystem respiration (Reco), and (g) forest floor respiration (Rff) of the years when a CSAD event occurred (2015, 2018 and 2022) against the respective long-term means (a, c, e, g). The grey bands around the long-term means represent the standard error of the respective long-term mean CO_2 fluxes. Soil respiration (SR) measurements are given as daily means (± SD) measured manually in 2022 only. Thicker lines represent CSAD events. The right panels (b, d, f, h) show the cumulative difference between the actual fluxes recorded during a CSAD event and the respective long-term mean fluxes (2005-2022 for NEP, GPP and Reco; 2019-2021 for Rff); the associated error bars show the cumulative standard errors of the long-term mean CO_2 fluxes for the respective CSAD event.

3.3 Drivers of NEP and Rff in 2015, 2018 and 2022

3.3.1 Comparison of drivers during the 2015, 2018, and 2022 with the long-term means

Daily mean NEP (NEP) during the growing seasons in 2015 and 2018 were mainly driven by daily mean incoming solar radiation (Rg), similar to the long-term daily mean NEP during 2005-2022 (Figure 4a). However, NEP during the 2022 growing season was more strongly driven by daily mean SWC than by Rg, as indicated by its high CVI (Figure 4a). Daily mean Tair and VPD were the second most important drivers of NEP in 2015 and 2018, with a CVI higher than the ones for the long-term mean 2005-2022. In contrast to NEP, daily mean Rff during the growing seasons 2019-2021 was mainly driven by daily mean

SWC, followed by daily mean $Tair_{ff}$ and TS (Figure 4b). We found that daily mean SWC was the main driver of Rff in 2018, with a much higher CVI compared to those of other years, followed by daily mean TS. Overall, the CVI of all variables was much lower in 2022 compared to those of the other years (Figure 4b).

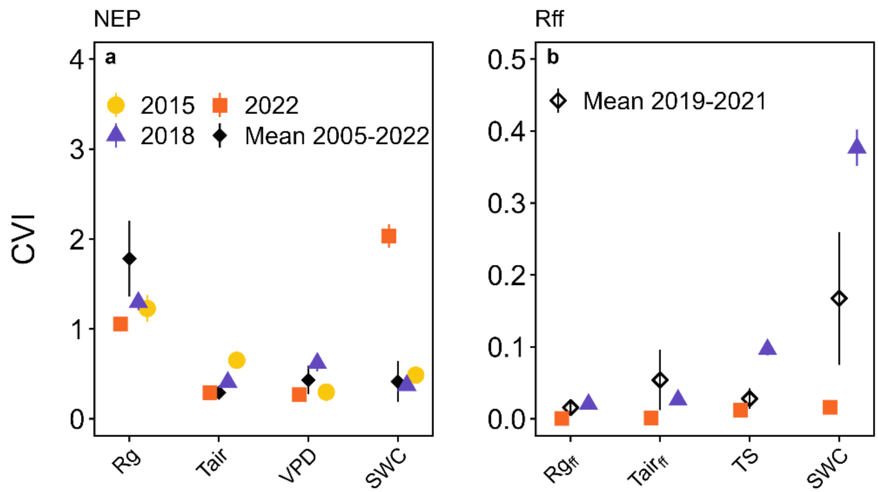

Figure 4. Driver analysis for daily mean (a) net ecosystem production (NEP) and (b) forest floor respiration (Rff) for the growing seasons 2015, 2018, 2022, compared with the long-term daily mean NEP 2005-2022 and the long-term daily mean Rff 2019-2021 calculated for each year separately. Note: Rff was not measured in 2015. The effect of driver (feature) variables is given by their conditional variable importance (CVI); Rg (incoming solar radiation), Tair (air temperature), VPD (vapor pressure deficit) and SWC (soil water content) were considered.

3.3.2 Temporal development of important drivers of daytime NEP and daily Rff

Testing the temporal development of the main drivers on daytime NEP with SHAP analysis revealed that overall, SWC, VPD and Tair decreased NEP during all CSAD events (Figure 5), while Rg increased daytime NEP. During the two CSAD events in 2015, both Tair and VPD were always associated with a decrease in NEP, while SWC exhibited a less consistent pattern, increasing NEP during the first CSAD event and decreasing NEP during the second (Figure 5a). Nevertheless, the mean contributions of Tair, SWC and VPD to NEP_{DT} during the CSAD events of 2015 were negative, with Tair having the largest effect in reducing NEP (Figure 5a). As stated previously, Rg enhanced NEP_{DT} in both CSAD events of 2015, contributing positively to NEP (Figure 5a). During the CSAD event of 2018, the mean contributions of Tair, VPD and SWC to NEP_{DT} were also all negative, leading to a decrease in NEP (Figure 5b). In contrast to 2015, SWC showed the largest negative effect on daytime NEP during the 2018 CSAD event, although it had clear positive effects prior to the CSAD onset. Rg both enhanced and decreased NEP_{DT} during the CSAD event of 2018, which resulted in a small mean positive contribution (Figure 5b). As observed for 2018, the mean contributions of Tair, VPD and SWC were all negative during the CSAD event of 2022, leading to a decrease in NEP (Figure 5c). Similarly to 2018, prior to the 2022 CSAD, SWC had a positive effect on daytime NEP, but then contributed the most to the decrease in NEP during the 2022 CSAD. As observed previously, Rg increased daytime NEP also during the 2022 CSAD event, shown by its positive contribution (Figure 5c). Lastly, during the reference period 2005-

2022 (from 7th of July to 23rd of August), Tair, VPD and SWC affected daytime NEP negatively, although the contributions of VPD and SWC were close to zero (Figure 5d). In contrast, the mean contribution of Rg to NEP_{DT} was positive, resulting in an increase of NEP_{DT} during the reference period 2005-2022 (Figure 5d).

In accordance with the previous analysis for NEP, the decrease in daily Rff during both CSAD events of 2018 and 2022 was mainly driven by negative effects of SWC (Figure 6a, b). In contrast, TS increased Rff during both CSAD events, but with much larger effects during the CSAD in 2018 compared to that in 2022. This coincided with negative effects of SWC on Rff already starting in mid-June, one month prior to the 2018 CSAD event (Figure 6a), while during the 2022 CSAD event, SWC effects only became negative shortly before the 2022 event (Figure 6b). The effect of Rg_{ff} during both CSAD events in 2018 and 2022 was positive, but overall close to zero (Figure 6a, b). For comparison, during the reference period (from 14th of July to 23rd of August 2019-2021), TS had the largest positive effect on Rff compared to the CSAD events in 2018 and 2022, which persisted typically until September when senescence and leaf fall set in (Figure 6c). On the other hand, the effects of Rg_{ff} and SWC varied around zero throughout all reference period summers (June, July, and August) (Figure 6c). Overall, mean contributions to changes in Rff during the reference period 2019-2021 were dominated by positive effects by TS, and close to zero contributions of Rg_{ff} and SWC (Figure 6c).

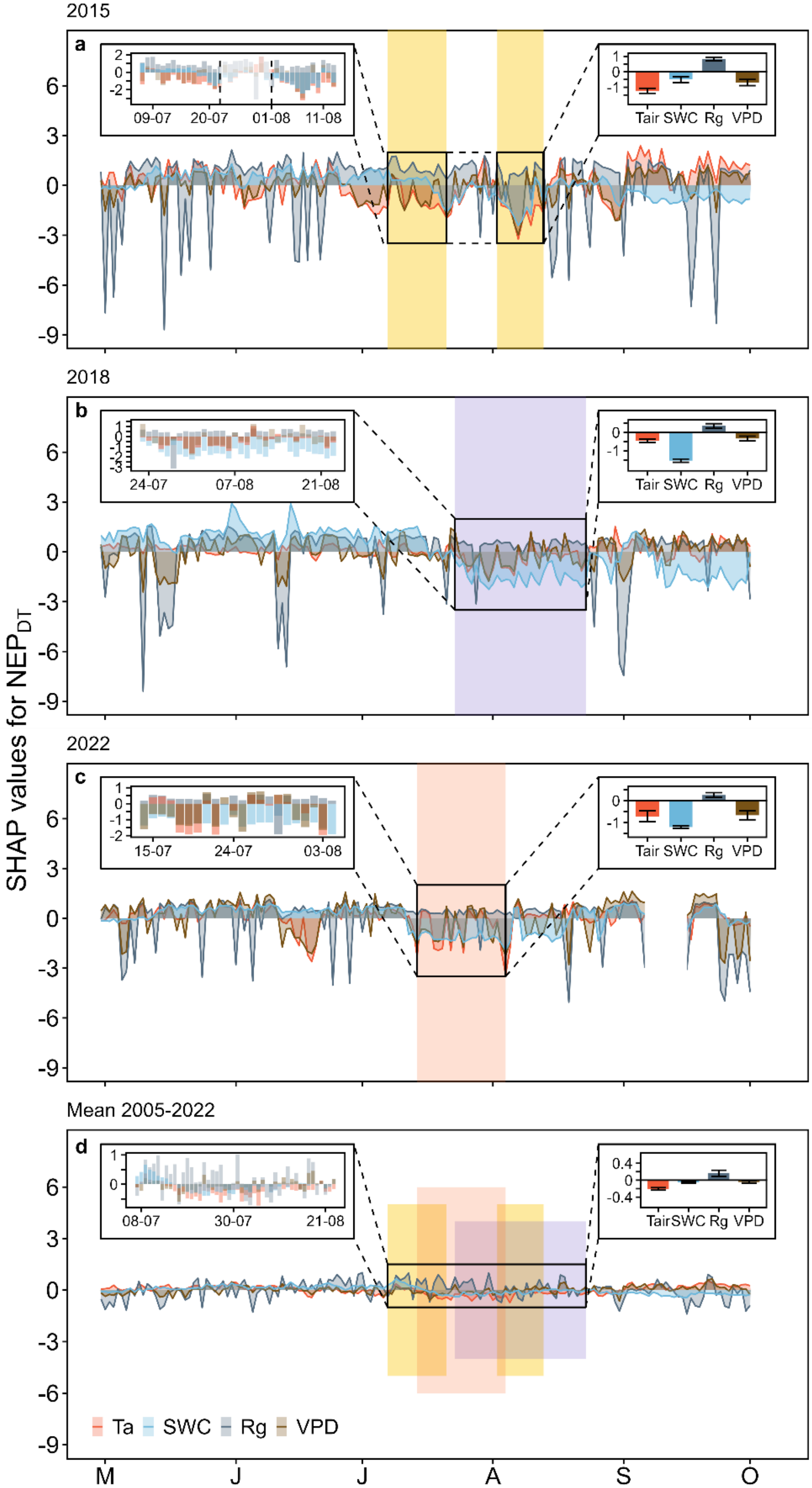
2015
a
09-07
20-07
01-08
11-08
Tair SWC Rg VPD
2018
b
24-07
07-08
21-08
Tair SWC Rg VPD
2022
c
15-07
24-07
03-08
Tair SWC Rg VPD
Mean 2005-2022
d
08-07
30-07
21-08
Tair SWC Rg VPD
Ta SWC Rg VPD
SHAP values for NEP_DT
M
J
J
A
S
O

Figure 5. Temporal course of feature contributions to daytime mean net ecosystem production (NEP) during the growing seasons of (a) 2015, (b) 2018, (c) 2022, and (d) the long-term mean (2005-2022), indicated by SHAP values for Tair, incoming radiation (Rg), VPD, and SWC. The small inserts on the left show the CSAD events (a-c) and the reference period for 2005-2022 (d). The small inserts on the right show mean (± SD) SHAP values for Tair, SWC, Rg and VPD during the CSAD events (a-c) and during the reference period for 2005-2022 (d). Positive SHAP values indicate positive effects on the response variable NEP, while negative SHAP values indicate negative effects. Coloured areas show the period in which a CSAD occurred in 2015, 2018 and 2022 (a-c); they are also shown in panel (d) to highlight the reference period for the long-term mean (2005-2022).

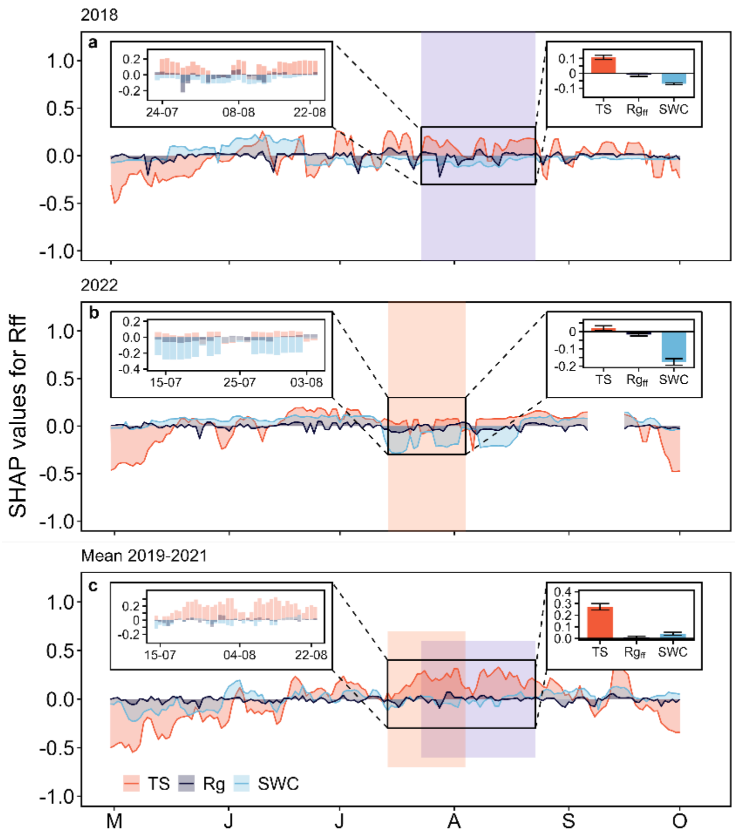

Figure 6. Temporal course of feature contributions to daily mean forest floor respiration (Rff) during the growing seasons of (a) 2018, (b) 2022, and (c) the non-CSAD years 2019-2021, indicated by SHAP values for soil temperature (TS), incoming radiation at the forest floor (Rg_{ff}), and SWC. The small inserts on the left show the CSAD events (a-b) and the reference period for 2019-2021 (from 14th July to 23rd August) (d). The small inserts on the right show mean (± SD) SHAP values for TS, Rg_{ff}, and SWC during the CSAD events (a-b) and during the reference period for 2019-2021 (c). Positive SHAP values indicate a positive effect on the response variable Rff, while negative SHAP values indicate negative effects. Coloured areas show the period in which a CSAD event occurred; they are also shown in panel (c) to highlight the reference period for 2019-2021.

3.3.3 Driver thresholds with largest effects on daytime mean NEP and daily mean Rff for the CSAD years

We derived thresholds for the drivers VPD, SWC, Tair, and TS to test if the absolute values of these drivers during the CSAD events actually differed from the absolute values that showed largest effects on NEP_{DT} or Rff (based on the maximum marginal contributions from SHAP analysis). Threshold values differed among the CSAD years, particularly for SWC_NEP_{max} and SWC_Rff_{max} which were positive in 2015 and 2018 but negative in 2022 (Table 3). VPD_NEP_{max} were relatively low for all CSAD years (between 0.7 and 0.8 kPA), while $Tair\_NEP_{max}$ increased from around 10 °C in 2015 to 13 °C in 2018 to 16 °C in 2022. For comparison, TS_Rff_{max} were around 19 °C in 2018 and 15.6 °C in 2022. Comparing measured driver values to those thresholds revealed that most daytime mean VPD values during the CSAD events were typically higher than the respective VPD_NEP_{max} threshold for each of the CSAD years, reaching values of up to 2.5 kPA (Figure 7a, d, g), only few exceptions occurred. In contrast, all daytime mean SWC values measured during the CSAD events were far below the SWC_NEP_{max} thresholds in all CSAD years (Figure 7b, e, h), resulting in very negative effects on daytime NEP. We also observed a decrease in SWC_NEP_{max} values from 2015 to 2022 (Figure 7b, e, h; Table 3). Likewise, daytime mean Tair measured during the CSAD events was far above the $Tair\_NEP_{max}$ threshold for all CSAD events (Figure 7c, f, i; Table 3). In addition, we observed an increase in $Tair\_NEP_{max}$ values from 2015 to 2022 (Figure 7c, f, i; Table 3). We also observed positive relationships between SWC_NEP_{max} and mean SWC as well as between VPD_NEP_{max} and mean VPD over the different growing seasons (Figure A5). Applying the same analysis to daily mean Rff (Figure 8) revealed that daily mean TS measured during the CSAD event in 2018 varied around the TS_Rff_{max} threshold of 2018 (Figure 8a), while measured TS values were higher than the TS_Rff_{max} threshold during the CSAD event in 2022 (Figure 8b). As observed for the NEP, SWC values measured during the CSAD events of 2018 and 2022 were far below the respective SWC_Rff_{max} thresholds (Figure 8b, d), with measured data as well as SWC_Rff_{max} thresholds being much lower in 2022 than in 2018 (Figure 8b, d; Table 3).

Table 3. Absolute driver thresholds (mean ± SE) related to the largest effect on NEP_{DT} or Rff during the three CSAD years and the long-term means (2005-2022 for NEP and 2019-2021 for Rff). Identification was based on the maximum marginal contribution of the respective driver (VPD, SWC, Tair and TS) in the SHAP analysis for each year.

Year	VPD_NEP_{max} (kPa)	SWC_NEP_{max} (normalised)	$Tair\_NEP_{max}$ (°C)	TS_Rff_{max} (°C)	SWC_Rff_{max} (normalised)
2015	0.66 ± 0.04	0.40 ± 0.43	9.79 ± 0.56	n.a.	n.a.
2018	0.84 ± 0.05	0.14 ± 0.6	13.13 ± 0.30	19.15 ± 0.07	0.58 ± 0.07
2022	0.77 ± 0.06	-0.86 ± 0.4	15.95± 0.37	15.60 ± 0.07	- 0.73 ± 0.09

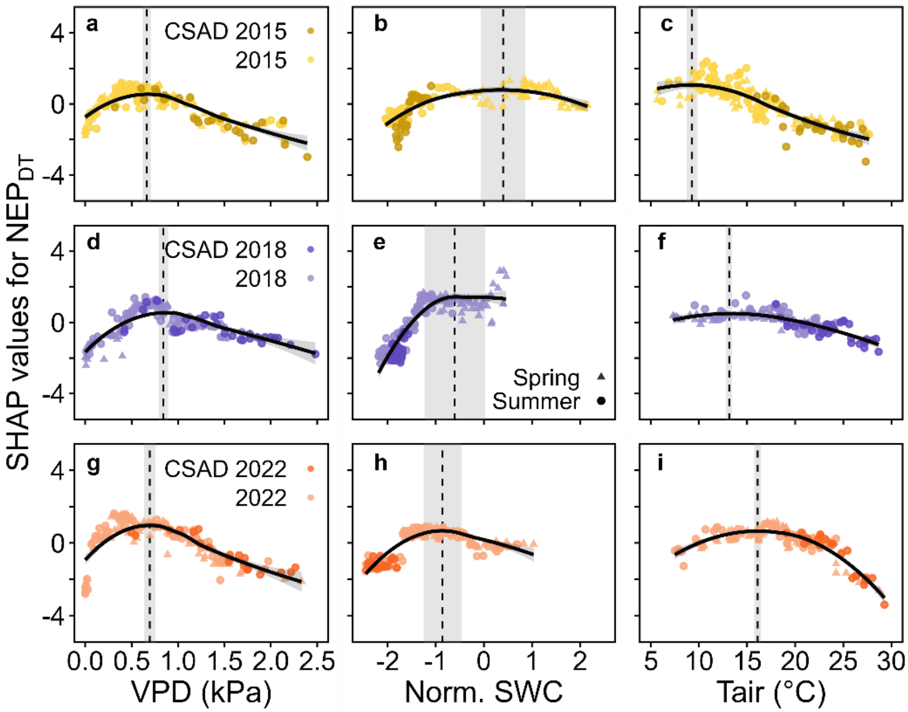

Figure 7. Detection of VPD, SWC and Tair values corresponding to the maximum rate of daytime mean net ecosystem production (NEP_{DT}) during the growing seasons of 2015, 2018 and 2022. Positive or negative SHAP values represent positive or negative effects on NEP_{DT}. The vertical dashed lines and the grey bands show VPD (a, d, g), SWC (b, e, h), and Tair (c, f, i) and their standard deviations, corresponding to the largest effect on NEP_{DT} based on the respective maximum marginal contribution of the respective driver in the SHAP analysis for each year to NEP for 2015, 2018 and 2022.

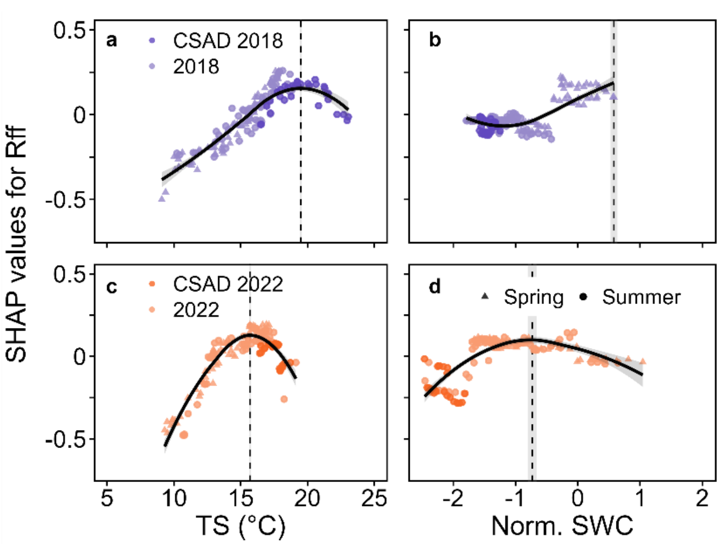

Figure 8. Detection of soil temperature (TS) and SWC values corresponding to the maximum rate of daily mean forest floor respiration (Rff) in 2018 and 2022. Positive or negative SHAP values represent positive or negative effects on Rff. The vertical dashed lines and grey bands show TS (a, c) and SWC (b, d) and their standard deviations, corresponding to the largest effect on Rff based

on the respective maximum marginal contribution of the respective driver in the SHAP analysis for each year to Rff in 2018 and 2022.

3.4 SR responses to TS and SWC in 2022

As seen above, daily mean SR rates mirrored the responses of Rff (Figure 3), though with a much coarser time resolution. The relationships of SR with TS and SWC varied, depending if CSAD events were considered or not (Figure 9). When no CSAD event was recorded, daily mean SR significantly increased with TS (R^2 = 0.76, P of 0.002; linear regression). However, during the CSAD event, SR did not respond to TS (R^2 = 0.19; Figure 9a). On the other hand, independent if a CSAD event was recorded or not, SR did not respond to variation in SWC (R^2 < 0.01 and R^2 = 0.3 respectively; Figure 9b).

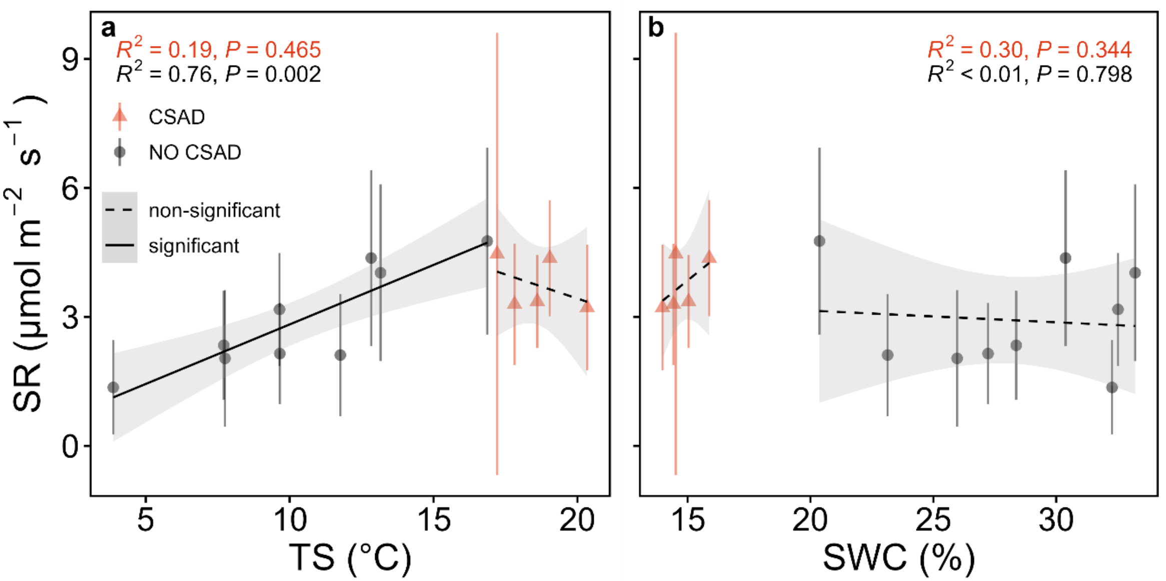

Figure 9. Linear relationships of daily mean soil respiration (SR) with (a) soil temperature (TS) and (b) soil water content (SWC) during the CSAD event 2022 and the rest of the year 2022. Two models were fitted separately for the periods with and without the CSAD event. The goodness of the fit is expressed with R^2 and p-values (P) in the respective panels according to the colour scale.

4 Discussion

In this study, we identified three compound soil and atmospheric drought (CSAD) events during the last 18 years (i.e., 2015, 2018, and 2022) for a mountain mixed deciduous forest. Although they were of comparable intensity, they differed in terms of their timing. We further assessed the mainly negative impacts of these CSAD events on ecosystem CO_2 fluxes (NEP, GPP, Reco) and forest floor respiration (Rff). Moreover, we quantified the temporal contribution of the main drivers to these fluxes during the CSAD events and the respective growing seasons (VPD, Tair, Rg, SWC, TS). Pronounced differences in driver effects as well as their temporal development were found for ecosystem vs. forest floor fluxes, but also among drivers and among CSAD events. In addition, we saw first signs of acclimation of NEP to such CSAD events, i.e., changed sensitivities of NEP to its drivers, both within the same and among different growing seasons. This also suggested that predictions of site-specific CSADs and their impacts might become more challenging in the future.

4.1 Compound soil and atmospheric drought (CSAD) events

Several recent studies have shown that Europe already did and also will experience an increase in intensity and frequency of CSAD conditions in the future (e.g., Shekhar et al., 2023; Markonis et al., 2021). Such increased occurrence of extremes was also evident during the 18 years (2005-2022) of eddy-covariance measurements at CH-Lae, with three years (2015, 2018, 2022) being characterized by CSAD events, all within the last eight years (2015-2022). Two other years, 2019 and 2020, also characterized by atmospheric drought, albeit at lower intensity than the three years identified here (Figure 1), did not show co-occurring soil drought at our forest site, and were therefore not classified as CSAD years. This nicely illustrated site-specific environmental conditions playing a relevant role when discussing the impact of extreme compound events at larger spatial scales (Shekhar et al., 2023). Interestingly, even though the intensities of the CSAD events of 2015, 2018 and 2022 were comparable in terms of SWC and VPD values, the pre-conditions and the time of occurrence were different. Pre-conditions (late-spring or early summer), especially in terms of soil moisture and temperature or VPD, can be wet and cool, near-normal, or dry and warm. Thus, depending on these pre-conditions, the impact of any CSAD event on forest performance will differ as shown here. Prior to a CSAD event, soil moisture plays a vital role in determining how well the forest can resist and also recover from the stress of a CSAD event (Jiao et al., 2021). Dry and warm vs. non-limiting conditions before the CSAD event can put the forest under additional water stress during the CSAD event, making it more susceptible to drought and heat stress (da Costa et al., 2018). However, even prior normal soil moisture and warm conditions in spring which favour productivity, but are also accompanied by increased water demands for evapotranspiration, lead to increased soil drying, and can thus amplify extreme dryness stress during summer drought as observed during the 2018 CSAD event at our mixed deciduous forest site (CH-Lae) and across Central Europe (Gharun et al., 2020; Bastos et al., 2020; Shekhar et al., 2020). Thus, CSAD events will require our full attention in the future, since their impacts will strongly differ not only depending on their frequency, duration, and intensity, but also depending on the prior site-specific environmental conditions the ecosystem experiences.

4.2 Forest CO_2 fluxes and their respective drivers

4.2.1 Net Ecosystem Productivity, NEP

The CSAD events of 2015, 2018 and 2022 resulted in a significant decrease in NEP, which was largely due to decreasing GPP (between 16 and 28%), while ecosystem respiration (Reco) either decreased or did not change compared to the long-term mean at the mixed deciduous forest. Such reductions in GPP during CSAD events have been observed in earlier studies, particularly for beech, the dominant species at our forest site (Ciais et al. 2005; Bastos et al., 2020; Dannenberg et al., 2022; D'Orangeville et al., 2018; Xu et al., 2020; Gharun et al., 2020). Increased stomatal closure in response to high VPD and low soil moisture (i.e., stomatal response), reduction of photosynthesis due to reduced carboxylation rate (Rubisco activity) at high temperatures (i.e., non-stomatal response; Buckley, 2019; Gourlez de la Motte et al., 2020) at leaf level as well as reduced canopy conductance at ecosystem level (Ciais et al. 2003, Granier et al. 2007, Gharun et al. 2020) are typically associated with such CSAD events.

Our driver analysis revealed that, among the considered features, air temperature had the largest effect on reducing NEP_{DT} during the CSAD event in 2015, but not in the others suggesting that stomatal responses on GPP were generally more relevant than temperature-related non-stomatal responses (Granier et al., 2007). Moreover, the major drivers we identified, i.e., VPD and SWC, support stomatal responses as underlying mechanisms for the reduction of net CO_2 uptake via GPP (Dannenberg et al., 2022; Fu et al., 2022; Petek-Petrik et al., 2023; van der Woude et al., 2023) during all CSAD events in 2015, 2018, and 2022. However, the contributions of those dryness-related variables varied among the CSAD events, suggesting that the response of the forest differed depending on the respective intensity of soil dryness (SWC) and of air dryness (VPD) during the CSAD events. Also, the conditions prior to the CSAD event seemed to play an important role, as SWC was more important for NEP during the 2022 CSAD event, which followed upon a prevailing soil drought, compared to the 2015 and 2018 CSAD events.

Another line of argumentation towards dryness-related vs. temperature-related drivers of reduced NEP during CSAD events is related to Reco with its two major components, i.e., plant and soil respiration. In our study, Reco was between 7-31% lower during the three CSAD years compared to the other years, supporting the dryness- over the temperature-related argumentation. While plant respiration typically increases in response to high temperatures (Schulze et al. 2019), it also depends on the intensity of the event: if substrate (i.e., carbohydrate) availability is diminished during a CSAD event due to reduced GPP, respiration can also decrease (Janssens et al. 2001; Ciais et al., 2005; Von Buttlar et al., 2018), albeit typically less than GPP (Schwalm et al. 2010). Similarly, soil respiration decreases when substrate supply for root and microbial respiration is low (Högberg et al. 2001; Ruehr et al. 2009). Moreover, soil respiration is known to be small when soil moisture is low (due to reduced microbial and root respiration) during CSAD events (Ruehr et al. 2010; Von Buttlar et al., 2018; Wang et al., 2014), as seen at our site in 2022. In addition to the standard response of NEP (and its components GPP and Reco) to abiotic drivers (VPD, SWC and Tair), NEP sensitivity to those drivers could change from one growing season to another (Grossman, 2023), especially during drought conditions, indicating acclimation of NEP (Crous et al., 2022; Aspinwall et al., 2017; Sendall et al., 2015; Sperlich et al., 2019). This difference in NEP sensitivity to VPD, SWC and Tair during the 2015, 2018, and 2022 growing seasons was clearly observed in our study (see response curves in Figure 7). The thresholds derived from the response curves of SHAP values vs. the abiotic drivers (Figure 7) indicated acclimation of NEP to higher VPD (in 2018 and 2022), and lower SWC (in 2022), as we observed a shift towards drier conditions of the VPD, and SWC values corresponding to the maximum marginal contribution of the features to NEP_{DT} in CSAD years (Figure 7, A5). Such drought acclimations could be due to biophysical adjustments such as access of soil water from deeper soil layers (Brinkmann et al., 2019), changes in photosynthetic thermal acclimation and changes in stomatal sensitivity to VPD (Aspinwall et al., 2017; Smith and Dukes, 2017; Gessler et al., 2020). Such NEP acclimation to higher VPD and lower SWC will be critical in the future, enabling forests to persist (longer) during CSAD events (Kumarathunge et al., 2019).

4.2.2 Forest floor and soil respiration, Rff and SR

The CSAD event in 2022 resulted in a more pronounced and rapid decrease of Rff than in 2018, leading to smaller CO_2 losses from the forest floor compared to 2018 CSAD and the reference period 2019-2021. We observed a similar seasonal trend of Rff and SR, but SR was consistently higher than Rff (Figure 3d). Rff is indeed composed by soil and understory vegetation respiration. At the CH-Lae site, the understory LAI (Leaf Area Index) decreased in late spring (Paul-Limoges, 2017) when trees leaf out, and light reaching the forest floor diminishes. Thus, during the growing season, most of the respiratory CO_2 fluxes from below the canopy consist of SR. Yet, a small part of the SR can be offset by photosynthesis of the vegetation still growing below the canopy (i.e., seedlings of *Fagus sylvatica* and other herbaceous plants). As we observed that GPP_{ff} was not different from zero during the growing seasons (Figure A6), we here assumed the effect of photosynthesis in the daily Rff being negligible. European mixed forests are usually more resistant to drought than monospecific ones in terms of microbial soil respiration (Gillespie et al., 2020). For example, Gillespie et al. (2020) found that CO_2 emissions were not decreasing under drought in natural mixed Europ ean forests. However, a reduction of SR during drought has been widely reported in other studies (e.g., Ruehr et al., 2010; Schindlbacher et al., 2012; Wang et al., 2014; Sun et al., 2019), but the interplay of intensity, duration, and biotic components can trigger different responses of the forest floor in the respective ecosystems (Talmon et al., 2011; Jiao et al., 2021).

The decreased importance of TS during the CSAD event of 2018 and 2022 compared to the reference period 2019-2021 (Figure 6) was driven by the limitation of Rff and SR by SWC. In accordance with the SR analysis, we found no effect of TS during the CSAD event in 2022 (Figure 9). Drought periods in forests can indeed diminish the temperature sensitivity of the SR (Jassal et al., 2008; Ruehr et al. 2010; Sun et al., 2019; Schindlbacher et al., 2012; van Straaten et al., 2011; Wang et al., 2014). Generally, SWC is not limiting at the CH-Lae site, but exceptions can occur during summer (Knohl et al., 2008; Ruehr et al., 2010; Trabucco and Zomer, 2022). We know that SR is the sum of heterotrophic and autotrophic respiration (Ruehr and Buchmann, 2009; Wang et al., 2014; Zheng et al., 2021). A large component of heterotrophic respiration is microbial activity in the soil. Under drought, the microbial activity is typically reduced by the limited diffusion of soluble carbon substrate for extracellular enzymes (Manzoni et al., 2012). Consequently, litter decomposition rates also decrease (Deng et al., 2021). If decomposition rates decrease, soil organic matter increases in the soil, resulting in higher C and N in the soil (van der Molen et al., 2011). At the same time, drought reduces photosynthesis and so plants tend to keep non-structural carbohydrates in the leaves or roots to sustain the living tissues (Högberg et al., 2008). Thereby, root activity and production are downregulated (Deng et al., 2021), which can lead to a decoupling of photosynthetic and underground activities (Ruehr et al., 2009; Barba et al., 2018). Eventually, soil drought can significantly alter the N and C cycle in the ecosystem (Deng et al., 2021).

The TS and SWC at which Rff_{max} was observed varied from growing season to growing season, as we saw for 2018 and 2022 (Figure 8). The SWC recorded during the CSAD events was clearly below SWC_Rff_{max}, but the TS recorded during the CSAD events was observed to be in the range of TS_Rff_{max} in 2018. The interplay and the seasonal trends of TS and SWC can thus determine at which abiotic conditions the highest respiration rate is found. Even though SR is projected to increase under global warming (Schindlbacher et al., 2012), the more frequent occurrence of droughts (Grillakis, 2019) could partially offset those emissions (Zheng et al., 2021), as we observed in the decrease of Rff during CSAD events. However, the decrease in CO_2 emissions can be compensated by CO_2 bursts from rain events occurring after drought periods (Lee et al., 2002) as we observed after the CSAD event in 2022 (Figure 3d). In general, a recovery of SR is expected if soil moisture quickly returns to normal conditions (Yao et al., 2023). Yet, biotic factors like fine roots are crucial for tree recovery after drought (Netzer et al., 2016; Hikino et al., 2021; Hikino et al., 2022). For example, it is well known that the fine roots of *Fagus sylvatica* can grow to deeper soil depths during drought, but only if the drought is not too severe, when they can be shed (Hildebrandt, et al., 2020). Indeed, Nickel et al., (2017) found a progressive decrease in vital fine roots after repeated drought in a mixed deciduous forest in Europe. Hence, the pre-and post-conditions, the timing, the intensity, and the duration of a CSAD are very important to predict the consequences in terms of respiratory CO_2 emissions.

5 Conclusions

For our mixed deciduous forest, we found first signs of NEP acclimation to more extreme soil (low SWC) and atmospheric drought (high VPD) conditions when comparing sensitivities of NEP to these drivers during the same growing season, which will be fundamental for drought resistance in the future. Nevertheless, we expect to witness a larger reduction of GPP with more extreme CSAD events in the future, even if complemented by a reduction in Reco. Hence responses to CSAD events might lead to a reduction of the CO_2 sink capacity of the forest in the future. The study also highlighted different behaviours of the responses of above-canopy and forest floor CO_2 fluxes during CSAD events. With further global warming in Europe, we expect an increase in Rff, but with more extreme droughts and more intense precipitation events, we assume a higher variability of the CO_2 emissions from forest soils and thus uncertain consequences for the respective soil carbon stocks. Ultimately, the consequences of CSAD events will influence the annual carbon budget of a forest, and thus jeopardising many restoration/reforestation projects or nature-based solutions as proposed in the Paris Agreement.

Appendix A

Table A1. List of instruments, models and manufacturers used in this study.

Instrument	Model	Manufacturer
Infrared gas analyser (IRGA)[1]	LI-7500 (2004-2015)	LI-COR Inc., Lincoln, NE, USA
Infrared gas analyser (IRGA)[1]	LI-7200 (2016-2022)	LI-COR Inc., Lincoln, NE, USA
3-D Sonic anemometer[1]	HS-50	Gill Instruments Ltd., Lymington, UK
Air temperature and relative humidity[2]	Rotronic MP 101 A	Rotronic AG, Bassersdorf, Switzerland
Incoming radiation[2]	BF2_BF2116	Delta-T Devices Ltd, Cambridge, UK
Infrared gas analyser (IRGA)[3]	LI-7500	LI-COR Inc., Lincoln, NE, USA
3-D Sonic anemometer[3]	R-350	Gill Instruments Ltd., Lymington, UK
Air temperature and relative humidiy[4]	CS215_E16511	Campbell Scientific Ltd., UG, USA
Soil temperature and water content[5]	Decagon ECH2O EC-20 probes (2004-2020)	Pullman, WA, USA
Soil temperature and water content[5]	TEROS 12_00007171 (2020-2022)	METER Group AG, NE, USA
Incoming radiation[4]	LI190SB-L	LI-COR Inc., Lincoln, NE, USA
Infrared gas analyser (IRGA)[6]	LI-8100	LI-COR Inc., Lincoln, NE, USA
Soil temperature[6]	GTH 175 PT	GHM Messtechnik GmbH, Regenstauf, Germany
Soil water content[6]	HH2 Moisture Meter	Delta-T Devices, Cambridge, United Kingdom

[1]Above-canopy EC system (47 m height)

[2]Above-canopy meteorological measurements (54 m height)

[3]Below-canopy EC system (1.5 m height)

[4]Below-canopy meteorological station (2 m height)

[5]Forest floor meteorological station (profile measurements at 5, 10, 20, 30, 50 cm depth)

[6]Portable sensors (SR survey measurements)

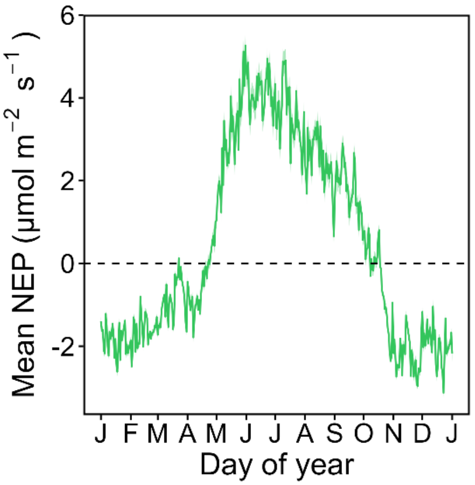

Figure A1. Long-term (2005-2022) daily mean and standard deviation of net ecosystem productivity (NEP) of CH-Lae. The zero-line highlights whether the daily NEP is positive or negative. The growing season was identified as the period in which daily NEP was positive (1st May to 31st September).

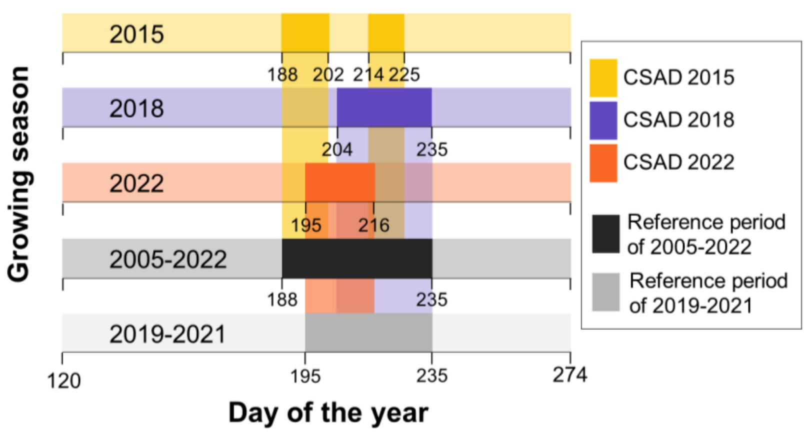

Figure A2. Graphical definition of reference periods. The five horizontal bars display the three growing seasons in which a CSAD event occurred, and the two long term means used as reference periods for comparison (2005-2022 for ecosystem level measurements and 2019-2021 for forest floor measurements). The CSAD periods are marked for each growing season in the CSAD years. The reference period of the mean 2005-2022 used in our analyses corresponds to the interval of time between day 188 (7th July) and day 235 (23rd of August), while the one of the mean 2019-2021 corresponds to the interval of time between day 195 (14th July) and day 235 (23rd of August).

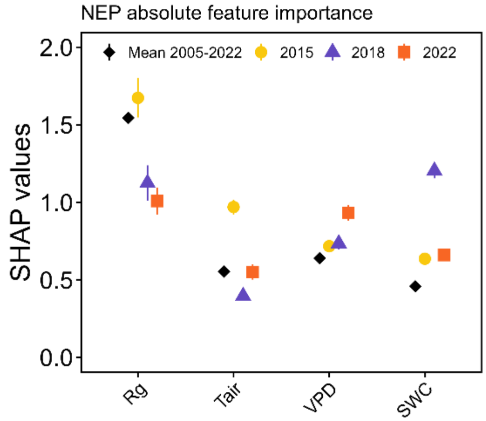

Figure A3. Absolute mean SHAP values (±SE) for daily mean NEP obtained with the XGBoost model.

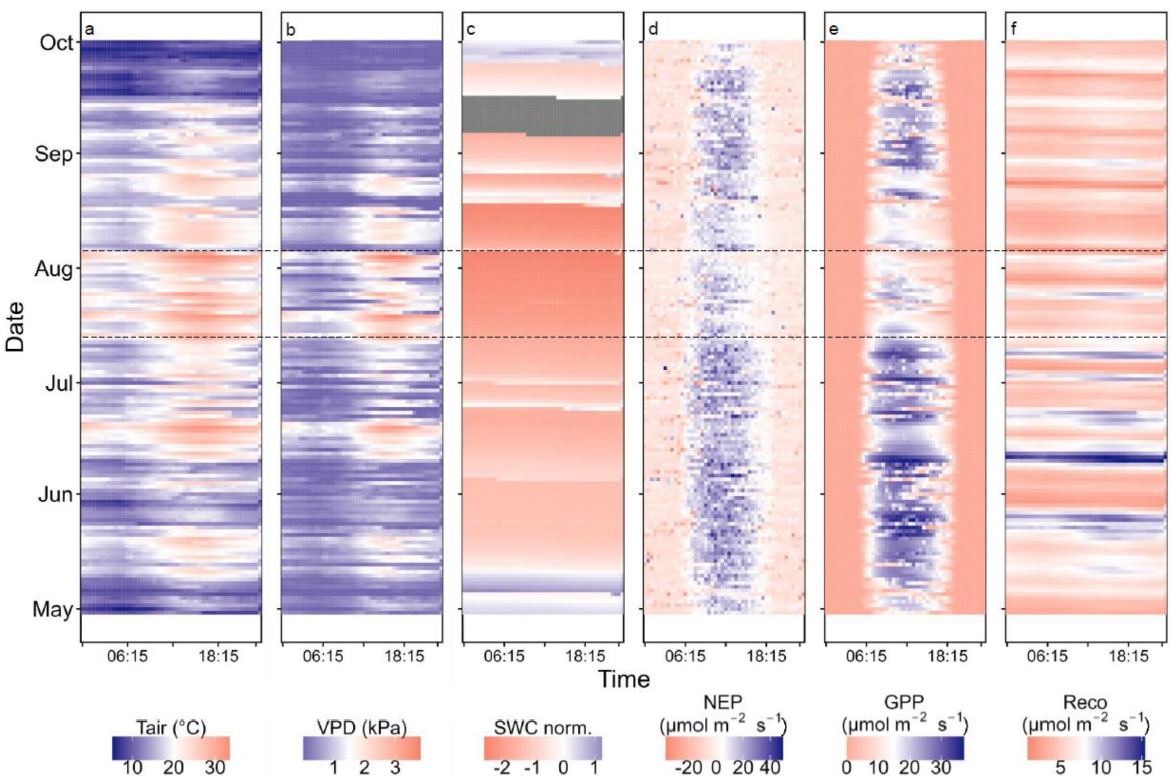

Figure A4. Diurnal (x-axis) and intra-annual (y-axis) variation of (a) air temperature (Tair), (b) VPD, (c) normalized soil water content (SWC at 20 cm depth) (d) net ecosystem production (NEP), (e) gross primary productivity (GPP), and (f) ecosystem respiration (Reco) during the 2022 growing season. 30 min averages are plotted in all panels. The two black dashed lines at 14th July 2022 and 4th August 2022 mark the compound soil and atmospheric drought (CSAD) event of summer 2022.

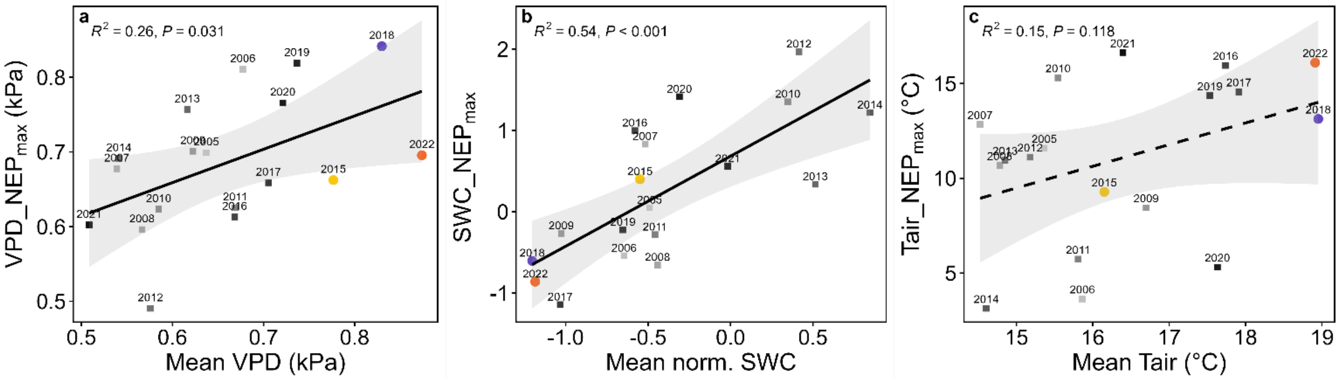

Figure A5. Linear regressions of mean VPD, SWC, and Tair values during the growing season of a given year against maximum marginal contributions of VPD, SWC and Tair (here abbreviated as feature_NEP$_{max}$) to daytime NEP. SWC values were normalized. The grey bands around the regression lines indicate the 95% confidence interval. R^2 and p-values are given as well.

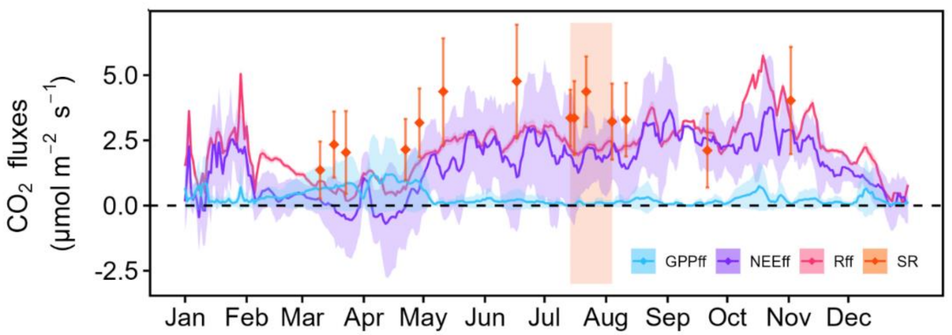

Figure A6. Forest floor CO_2 fluxes in 2022. The continuous lines show gap-filled and partitioned daily mean fluxes and standard deviations (coloured bands). 30 min averages are plotted. The diamonds represent daily means of manual soil respiration measurements, standard deviations are given as well. The area colored in orange represents the CSAD event of 2022.

Code availability

The R scripts used for data analyses and plots are available in the Git repository with the following link https://github.com/lscapucci/Compound-soil-and-atmospheric-drought-events-and-CO2-fluxes-of-a-mixed-deciduous-forest.

Author contribution

LS, AS, MG, NB conceptualization of the study, LS, AS, SAB, AB field campaigns, LS, AS, LH data processing and management, LS, AS data analyses; LS, AS, NB manuscript writing, all authors revision and editing of the manuscript.

Competing interests

The contact author has declared that none of the authors has any competing interests.

Acknowledgements

Authors acknowledge funding from the ETH Zürich project FEVER (ETH-27 19-1), and the SNF funded projects COCO (200021_197357), ICOS-CH Phase 3 (20F120_198227), and EcoDrive (IZCOZ0_198094), and the great support of the Grassland Sciences group members, especially Anna Katarina Gilgen, Luana Krebs, Julia Hauri, Franziska Richter, Yi Wang, Fabio Turco, Ruikun Gou, Roland Anton Werner, and Davide Andreatta.

References

Anderegg, W. R. L., Wu, C., Acil, N., Carvalhais, N., Pugh, T. A. M., Sadler, J. P., and Seidl, R.: A climate risk analysis of Earth's forests in the 21st century, Science, 377, 1099-1103, 10.1126/science.abp 9723, 2022.

Aspinwall, M. J., Vårhammar, A., Blackman, C. J., Tjoelker, M. G., Ahrens, C., Byrne, M., Tissue, D. T., and Rymer, P. D.: Adaptation and acclimation both influence photosynthetic and respiratory temperature responses in, Tree Physiology, 37, 1095-1112, 10.1093/treephys/tpx047, 2017.

Aubinet, M., Vesala, T., and Papale, D.: Eddy covariance: a practical guide to measurement and data analysis, Springer Science & Business Media2012.

Barba, J., Lloret, F., Poyatos, R., Molowny-Horas, R., and Yuste, J. C.: Multi-temporal influence of vegetation on soil respiration in a drought-affected forest, Iforest-Biogeosciences and Forestry, 11, 189-198, 10.3832/ifor2448-011, 2018.

Bastos, A., Ciais, P., Friedlingstein, P., Sitch, S., Pongratz, J., Fan, L., Wigneron, J. P., Weber, U., Reichstein, M., Fu, Z., Anthoni, P., Arneth, A., Haverd, V., Jain, A. K., Joetzjer, E., Knauer, J., Lienert, S., Loughran, T., McGuire, P. C., Tian, H., Viovy, N., and Zaehle, S.: Direct and seasonal legacy effects of the 2018 heat wave and drought on European ecosystem productivity, Science Advances, 6, 10.1126/sciadv.aba2724, 2020.

Birami, B., Gattmann, M., Heyer, A. G., Grote, R., Arneth, A., and Ruehr, N. K.: Heat Waves Alter Carbon Allocation and Increase Mortality of Aleppo Pine Under Dry Conditions, Frontiers in Forests and Global Change, 1, 10.3389/ffgc.2018.00008, 2018.

Bogati, K. and Walczak, M.: The Impact of Drought Stress on Soil Microbial Community, Enzyme Activities and Plants, Agronomy-Basel, 12, 10.3390/agronomy12010189, 2022.

Breiman, L.: Random forests, Machine Learning, 45, 5-32, Doi 10.1023/A:1010933404324, 2001.

Brinkmann, N., Eugster, W., Buchmann, N., and Kahmen, A.: Species-specific differences in water uptake depth of mature temperate trees vary with water availability in the soil, Plant Biology, 21, 71-81, 10.1111/plb.12907, 2019.

Buckley, T. N.: How do stomata respond to water status?, New Phytologist, 224, 21-36, 10.1111/nph.15899, 2019.

Chen, T. and Guestrin, C.: XGBoost: A Scalable Tree Boosting System, Proceedings of the 22nd ACM SIGKDD International Conference on Knowledge Discovery and Data Mining, San Francisco, California, USA, 10.1145/2939672.2939785, 2016.

Chi, J. S., Zhao, P., Klosterhalfen, A., Jocher, G., Kljun, N., Nilsson, M. B., and Peichl, M.: Forest floor fluxes drive differences in the carbon balance of contrasting boreal forest stands, Agricultural and Forest Meteorology, 306, 10.1016/j.agrformet.2021.108454, 2021.

Ciais, P., Reichstein, M., Viovy, N., Granier, A., Ogée, J., Allard, V., Aubinet, M., Buchmann, N., Bernhofer, C., Carrara, A., Chevallier, F., De Noblet, N., Friend, A. D., Friedlingstein, P., Grünwald, T., Heinesch, B., Keronen, P., Knohl, A., Krinner, G., Loustau, D., Manca, G., Matteucci, G., Miglietta, F., Ourcival, J. M., Papale, D., Pilegaard, K., Rambal, S., Seufert, G., Soussana, J. F., Sanz, M. J., Schulze, E. D., Vesala, T., and Valentini, R.: Europe-wide reduction in primary productivity caused by the heat and drought in 2003, Nature, 437, 529-533, 10.1038/nature03972, 2005.

Copernicus Climate Change Service: European State of the Climate 2019, https://climate.copernicus.eu/ESOTC/2019, 2019.

Copernicus Climate Change Service (C3S): European State of the Climate 2022, https://climate.copernicus.eu/esotc/2022, 2023.

Crous, K. Y., Uddling, J., and De Kauwe, M. G.: Temperature responses of photosynthesis and respiration in evergreen trees from boreal to tropical latitudes, New Phytologist, 234, 353-374, 10.1111/nph.17951, 2022.

da Costa, A. C. L., Rowland, L., Oliveira, R. S., Oliveira, A. A. R., Binks, O. J., Salmon, Y., Vasconcelos, S. S., Junior, J. A. S., Ferreira, L. V., Poyatos, R., Mencuccini, M., and Meir, P.: Stand dynamics modulate water cycling and mortality risk in droughted tropical forest, Global Change Biology, 24, 249-258, 10.1111/gcb.13851, 2018.

Dannenberg, M. P., Yan, D., Barnes, M. L., Smith, W. K., Johnston, M. R., Scott, R. L., Biederman, J. A., Knowles, J. F., Wang, X., Duman, T., Litvak, M. E., Kimball, J. S., Williams, A. P., and Zhang, Y.: Exceptional heat and atmospheric dryness amplified losses of primary production during the 2020 U.S. Southwest hot drought, Glob Chang Biol, 28, 4794-4806, 10.1111/gcb.16214, 2022.

de la Motte, L. G., Beauclaire, Q., Heinesch, B., Cuntz, M., Foltynová, L., Sigut, L., Kowalska, N., Manca, G., Ballarin, I. G., Vincke, C., Roland, M., Ibrom, A., Lousteau, D., Siebicke, L., Neiryink, J., and Longdoz, B.: Non-stomatal processes reduce gross primary productivity in temperate forest ecosystems during severe edaphic drought, Philosophical Transactions of the Royal Society B-Biological Sciences, 375, 10.1098/rstb.2019.0527, 2020.

Deng, L., Peng, C. H., Kim, D. G., Li, J. W., Liu, Y. L., Hai, X. Y., Liu, Q. Y., Huang, C. B., Shangguan, Z. P., and Kuzyakov, Y.: Drought effects on soil carbon and nitrogen dynamics in global natural ecosystems, Earth-Science Reviews, 214, 10.1016/j.earscirev.2020.103501, 2021.

Dirmeyer, P. A., Balsamo, G., Blyth, E. M., Morrison, R., and Cooper, H. M.: Land-atmosphere interactions exacerbated the drought and heatwave over northern Europe during summer 2018, AGU Advances, 2, e2020AV000283, 2021.

D'Orangeville, L., Maxwell, J., Kneeshaw, D., Pederson, N., Duchesne, L., Logan, T., Houle, D., Arseneault, D., Beier, C. M., Bishop, D. A., Druckenbrod, D., Fraver, S., Girard, F., Halman, J., Hansen, C., Hart, J. L., Hartmann, H., Kaye, M., Leblanc, D., Manzoni, S., Ouimet, R., Rayback, S., Rollinson, C. R., and Phillips, R. P.: Drought timing and local climate determine the sensitivity of eastern temperate forests to drought, Global Change Biology, 24, 2339-2351, 10.1111/gcb.14096, 2018.

Fan, S. M., Wofsy, S. C., Bakwin, P. S., Jacob, D. J., and Fitzjarrald, D. R.: Atmosphere-biosphere exchange of CO_2 and O_3 in the Central-Amazon-Forest, Journal of Geophysical Research-Atmospheres, 95, 16851-16864, DOI 10.1029/JD095iD10p16851, 1990.

Foken, T., Göockede, M., Mauder, M., Mahrt, L., Amiro, B., and Munger, W.: Post-field data quality control, in: Handbook of micrometeorology: a guide for surface flux measurement and analysis, Springer, 181-208, 2004.

Fratini, G., Ibrom, A., Arriga, N., Burba, G., and Papale, D.: Relative humidity effects on water vapour fluxes measured with closed-path eddy-covariance systems with short sampling lines, Agricultural and Forest Meteorology, 166, 234-234, 10.1016/j.agrformet.2012.10.013, 2012.

Gazol, A. and Camarero, J. J.: Compound climate events increase tree drought mortality across European forests, Science of the Total Environment, 816, 10.1016/j.scitotenv.2021.151604, 2022.

George, J. P., Bürkner, P. C., Sanders, T. G. M., Neumann, M., Cammalleri, C., Vogt, J. V., and Lang, M.: Long-term forest monitoring reveals constant mortality rise in European forests, Plant Biology, 24, 1108-1119, 10.1111/plb.13469, 2022.

Gessler, A., Bottero, A., Marshall, J., and Arend, M.: The way back: recovery of trees from drought and its implication for acclimation, New Phytologist, 228, 1704-1709, 10.1111/nph.16703, 2020.

Gharun, M., Hörtnagl, L., Paul-Limoges, E., Ghiasi, S., Feigenwinter, I., Burri, S., Marquardt, K., Etzold, S., Zweifel, R., Eugster, W., and Buchmann, N.: Physiological response of Swiss ecosystems to 2018 drought across plant types and elevation, Philosophical Transactions of the Royal Society B-Biological Sciences, 375, 10.1098/rstb.2019.0521, 2020.

Gillespie, L. M., Fromin, N., Milcu, A., Buatois, B., Pontoizeau, C., and Hättenschwiler, S.: Higher tree diversity increases soil microbial resistance to drought, Communications biology, 3, 377, 10.1038/s42003-020-1112-0, 2020.

Greco, S. and Baldocchi, D. D.: Seasonal variations of CO_2 and water vapour exchange rates over a temperate deciduous forest, Global Change Biology, 2, 183-197, 10.1111/j.1365-2486.1996.tb00071.x, 1996.

Grillakis, M. G.: Increase in severe and extreme soil moisture droughts for Europe under climate change, Science of The Total Environment, 660, 1245-1255, 10.1016/j.scitotenv.2019.01.001, 2019.

Grossiord, C., Buckley, T. N., Cernusak, L. A., Novick, K. A., Poulter, B., Siegwolf, R. T. W., Sperry, J. S., and McDowell, N. G.: Plant responses to rising vapor pressure deficit, New Phytologist, 226, 1550-1566, 10.1111/nph.16485, 2020.

Grossiord, C., Sevanto, S., Borrego, I., Chan, A. M., Collins, A. D., Dickman, L. T., Hudson, P. J., McBranch, N., Michaletz, S. T., Pockman, W. T., Ryan, M., Vilagrosa, A., and McDowell, N. G.: Tree water dynamics in a drying and warming world, Plant Cell and Environment, 40, 1861-1873, 10.1111/pce.12991, 2017.

Grossman, J. J.: Phenological physiology: seasonal patterns of plant stress tolerance in a changing climate, New Phytologist, 237, 1508-1524, 2023.

Haberstroh, S., Werner, C., Grün, M., Kreuzwieser, J., Seifert, T., Schindler, D., and Christen, A.: Central European 2018 hot drought shifts scots pine forest to its tipping point, Plant Biology, 24, 1186-1197, 10.1111/plb.13455, 2022.

Harris, N. L., Gibbs, D. A., Baccini, A., Birdsey, R. A., de Bruin, S., Farina, M., Fatoyinbo, L., Hansen, M. C., Herold, M., Houghton, R. A., Potapov, P. V., Suarez, D. R., Roman-Cuesta, R. M., Saatchi, S. S., Slay, C. M., Turubanova, S. A., and

Tyukavina, A.: Global maps of twenty-first century forest carbon fluxes, Nature Climate Change, 11, 10.1038/s41558-020-00976-6, 2021.
Hermann, M., Röthlisberger, M., Gessler, A., Rigling, A., Senf, C., Wohlgemuth, T., and Wernli, H.: Meteorological history of low-forest-greenness events in Europe in 2002-2022, Biogeosciences, 20, 1155-1180, 10.5194/bg-20-1155-2023, 2023.
Hikino, K., Danzberger, J., Riedel, V. P., Rehschuh, R., Ruehr, N. K., Hesse, B. D., Lehmann, M. M., Buegger, F., Weikl, F., Pritsch, K., and Grams, T. E. E.: High resilience of carbon transport in long-term drought-stressed mature Norway spruce trees within 2 weeks after drought release, Global Change Biology, 28, 2095-2110, 10.1111/gcb.16051, 2022.
Hikino, K., Danzberger, J., Riedel, V. P., Hesse, B. D., Hafner, B. D., Gebhardt, T., Rehschuh, R., Ruehr, N. K., Brunn, M., Bauerle, T. L., Landhäusser, S. M., Lehmann, M. M., Rötzer, T., Pretzsch, H., Buegger, F., Weikl, F., Pritsch, K., and Grams, T. E. E.: Dynamics of initial carbon allocation after drought release in mature Norway spruce-Increased belowground allocation of current photoassimilates covers only half of the carbon used for fine-root growth, Global Change Biology, 28, 6889-6905, 10.1111/gcb.16388, 2022.
Hildebrandt, A.: Root-water relations and interactions in mixed forest settings, Forest-Water Interactions, 240, 319-348, 10.1007/978-3-030-26086-6_14, 2020.
Högberg, P., Nordgren, A., Buchmann, N., Taylor, A. F. S., Ekblad, A., Högberg, M. N., Nyberg, G., Ottosson-Löfvenius, M., and Read, D. J.: Large-scale forest girdling shows that current photosynthesis drives soil respiration, Nature, 411, 789-792, Doi 10.1038/35081058, 2001.
Högberg, P., Högberg, M. N., Göttlicher, S. G., Betson, N. R., Keel, S. G., Metcalfe, D. B., Campbell, C., Schindlbacher, A., Hurry, V., Lundmark, T., Linder, S., and Näsholm, T.: High temporal resolution tracing of photosynthate carbon from the tree canopy to forest soil microorganisms, New Phytologist, 177, 220-228, 10.1111/j.1469-8137.2007.02238.x, 2008.
Horst, T. W.: A simple formula for attenuation of eddy fluxes measured with first-order-response scalar sensors, Boundary-Layer Meteorology, 82, 219-233, Doi 10.1023/A:1000229130034, 1997.
Hothorn, T., Hornik, K., and Zeileis, A.: Unbiased recursive partitioning: A conditional inference framework, Journal of Computational and Graphical Statistics, 15, 651-674, 10.1198/106186006x133933, 2006.
Intergovernmental Panel on Climate, C.: Climate Change 2022 – Impacts, Adaptation and Vulnerability: Working Group II Contribution to the Sixth Assessment Report of the Intergovernmental Panel on Climate Change, Cambridge University Press, Cambridge, 10.1017/9781009325844, 2023.
Ionita, M., Dima, M., Nagavciuc, V., Scholz, P., and Lohmann, G.: Past megadroughts in central Europe were longer, more severe and less warm than modern droughts, Communications Earth & Environment, 2, 10.1038/s43247-021-00130-w, 2021.
Ionita, M., Tallaksen, L. M., Kingston, D. G., Stagge, J. H., Laaha, G., Van Lanen, H. A. J., Scholz, P., Chelcea, S. M., and Haslinger, K.: The European 2015 drought from a climatological perspective, Hydrology and Earth System Sciences, 21, 1397-1419, 10.5194/hess-21-1397-2017, 2017.

Janssens, I. A., Lankreijer, H., Matteucci, G., Kowalski, A. S., Buchmann, N., Epron, D., Pilegaard, K., Kutsch, W., Longdoz, B., Grünwald, T., Montagnani, L., Dore, S., Rebmann, C., Moors, E. J., Grelle, A., Rannik, Ü., Morgenstern, K., Oltchev, S., Clement, R., Gudmundsson, J., Minerbi, S., Berbigier, P., Ibrom, A., Moncrieff, J., Aubinet, M., Bernhofer, C., Jensen, N. O., Vesala, T., Granier, A., Schulze, E. D., Lindroth, A., Dolman, A. J., Jarvis, P. G., Ceulemans, R., and Valentini, R.: Productivity overshadows temperature in determining soil and ecosystem respiration across European forests, Global Change Biology, 7, 269-278, 10.1046/j.1365-2486.2001.00412.x, 2001.

Jassal, R. S., Black, T. A., Novak, M. D., Gaumont-Guay, D., and Nesic, Z.: Effect of soil water stress on soil respiration and its temperature sensitivity in an 18-year-old temperate Douglas-fir stand, Global Change Biology, 14, 1305-1318, 10.1111/j.1365-2486.2008.01573.x, 2008.

Jiao, T., Williams, C. A., De Kauwe, M. G., Schwalm, C. R., and Medlyn, B. E.: Patterns of post-drought recovery are strongly influenced by drought duration, frequency, post-drought wetness, and bioclimatic setting, Global Change Biology, 27, 4630-4643, 10.1111/gcb.15788, 2021.

Kim, J. B., So, J. M., and Bae, D. H.: Global Warming impacts on severe drought characteristics in Asia monsoon region, Water, 12, 10.3390/w12051360, 2020.

Kittler, F., Eugster, W., Foken, T., Heimann, M., Kolle, O., and Göckede, M.: High-quality eddy-covariance CO_2 budgets under cold climate conditions, Journal of Geophysical Research-Biogeosciences, 122, 2064-2084, 10.1002/2017jg003830, 2017.

Knohl, A., Soe, A. R. B., Kutsch, W. L., Göckede, M., and Buchmann, N.: Representative estimates of soil and ecosystem respiration in an old beech forest, Plant and Soil, 302, 189-202, 10.1007/s11104-007-9467-2, 2008.

Körner, C., Möhl, P., and Hiltbrunner, E.: Four ways to define the growing season, Ecology Letters, 10.1111/ele.14260, 2023.

Kumarathunge, D. P., Medlyn, B. E., Drake, J. E., Tjoelker, M. G., Aspinwall, M. J., Battaglia, M., Cano, F. J., Carter, K. R., Cavaleri, M. A., Cernusak, L. A., Chambers, J. Q., Crous, K. Y., De Kauwe, M. G., Dillaway, D. N., Dreyer, E., Ellsworth, D. S., Ghannoum, O., Han, Q. M., Hikosaka, K., Jensen, A. M., Kelly, J. W. G., Kruger, E. L., Mercado, L. M., Onoda, Y., Reich, P. B., Rogers, A., Slot, M., Smith, N. G., Tarvainen, L., Tissue, D. T., Togashi, H. F., Tribuzy, E. S., Uddling, J., Vårhammar, A., Wallin, G., Warren, J. M., and Way, D. A.: Acclimation and adaptation components of the temperature dependence of plant photosynthesis at the global scale, New Phytologist, 222, 768-784, 10.1111/nph.15668, 2019.

Lal, P., Shekhar, A., Gharun, M., and Das, N. N.: Spatiotemporal evolution of global long-term patterns of soil moisture, Science of the Total Environment, 867, 10.1016/j.scitotenv.2023.161470, 2023.

Lasslop, G., Reichstein, M., Papale, D., Richardson, A. D., Arneth, A., Barr, A., Stoy, P., and Wohlfahrt, G.: Separation of net ecosystem exchange into assimilation and respiration using a light response curve approach: critical issues and global evaluation, Global Change Biology, 16, 187-208, 10.1111/j.1365-2486.2009.02041.x, 2010.

Lee, M.-s., Nakane, K., Nakatsubo, T., Mo, W.-h., and Koizumi, H.: Effects of rainfall events on soil CO 2 flux in a cool temperate deciduous broad-leaved forest, Ecological Research, 17, 401-409, 10.1046/j.1440-1703.2002.00498.x, 2002.

Lloyd, J. and Taylor, J. A.: On the temperature-dependence of soil respiration, Functional Ecology, 8, 315-323, 10.2307/2389824, 1994.

Lu, R. Y., Xu, K., Chen, R. D., Chen, W., Li, F., and Lv, C. Y.: Heat waves in summer 2022 and increasing concern regarding heat waves in general, Atmospheric and Oceanic Science Letters, 16, 10.1016/j.aosl.2022.100290, 2023.

Lundberg, S. M. and Lee, S. I.: A Unified Approach to interpreting model predictions, advances in neural information processing systems, 30, 2017.

Lundberg, S. M., Erion, G., Chen, H., DeGrave, A., Prutkin, J. M., Nair, B., Katz, R., Himmelfarb, J., Bansal, N., and Lee, S. I.: From local explanations to global understanding with explainable AI for trees, Nature Machine Intelligence, 2, 56-67, 10.1038/s42256-019-0138-9, 2020.

Manzoni, S., Schimel, J. P., and Porporato, A.: Responses of soil microbial communities to water stress: results from a meta-analysis, Ecology, 93, 930-938, Doi 10.1890/11-0026.1, 2012.

Markonis, Y., Kumar, R., Hanel, M., Rakovec, O., Máca, P., and AghaKouchak, A.: The rise of compound warm-season droughts in Europe, Science Advances, 7, 10.1126/sciadv.abb9668, 2021.

Martinez-Garcia, E., Nilsson, M. B., Laudon, H., Lundmark, T., Fransson, J. E. S., Wallerman, J., and Peichl, M.: Overstory dynamics regulate the spatial variability in forest-floor CO_2 fluxes across a managed boreal forest landscape, Agricultural and Forest Meteorology, 318, 10.1016/j.agrformet.2022.108916, 2022.

Mauder, M. and Foken, T.: Impact of post-field data processing on eddy covariance flux estimates and energy balance closure, Meteorologische Zeitschrift, 15, 597-610, 2006.

MeteoSvizzera. (2023). Rapporto sul clima 2022.

Miralles, D. G., Gentine, P., Seneviratne, S. I., and Teuling, A. J.: Land-atmospheric feedbacks during droughts and heatwaves: state of the science and current challenges, Annals of the New York Academy of Sciences, 1436, 19-35, 10.1111/nyas.13912, 2019.

Moncrieff, J., Clement, R., Finnigan, J., and Meyers, T.: Averaging, detrending, and filtering of eddy covariance time series, in: Handbook of micrometeorology: A guide for surface flux measurement and analysis, Springer, 7-31, 2004.

Moravec, V., Markonis, Y., Rakovec, O., Svoboda, M., Trnka, M., Kumar, R., and Hanel, M.: Europe under multi-year droughts: how severe was the 2014-2018 drought period?, Environmental Research Letters, 16, 10.1088/1748-9326/abe828, 2021.

Netzer, F., Thöm, C., Celepirovic, N., Ivankovic, M., Alfarraj, S., Dounavi, A., Simon, J., Herschbach, C., and Rennenberg, H.: Drought effects on C, N, and P nutrition and the antioxidative system of beech seedlings depend on geographic origin, Journal of Plant Nutrition and Soil Science, 179, 136-150, 10.1002/jpln.201500461, 2016.

Nickel, U. T., Weikl, F., Kerner, R., Schäfer, C., Kallenbach, C., Munch, J. C., and Pritsch, K.: Quantitative losses vs. qualitative stability of ectomycorrhizal community responses to 3 years of experimental summer drought in a beech-spruce forest, Global Change Biology, 24, E560-E576, 10.1111/gcb.13957, 2018.

Obladen, N., Dechering, P., Skiadaresis, G., Tegel, W., Kessler, J., Höllerl, S., Kaps, S., Hertel, M., Dulamsuren, C., Seifert, T., Hirsch, M., and Seim, A.: Tree mortality of European beech and Norway spruce induced by 2018-2019 hot droughts in central Germany, Agricultural and Forest Meteorology, 307, 10.1016/j.agrformet.2021.108482, 2021.

Orth, R.: When the land surface shifts gears, AGU Advances, 2, 10.1029/2021AV000414, 2021.

Paul-Limoges, E., Wolf, S., Eugster, W., Hörtnagl, L., and Buchmann, N.: Below-canopy contributions to ecosystem CO_2 fluxes in a temperate mixed forest in Switzerland, Agricultural and Forest Meteorology, 247, 582-596, 10.1016/j.agrformet.2017.08.011, 2017.

Paul-Limoges, E., Wolf, S., Schneider, F. D., Longo, M., Moorcroft, P., Gharun, M., and Damm, A.: Partitioning evapotranspiration with concurrent eddy covariance measurements in a mixed forest, Agricultural and Forest Meteorology, 280, 10.1016/j.agrformet.2019.107786, 2020.

Pei, F. S., Li, X., Liu, X. P., and Lao, C. H.: Assessing the impacts of droughts on net primary productivity in China, Journal of Environmental Management, 114, 362-371, 10.1016/j.jenvman.2012.10.031, 2013.

Petek-Petrik, A., Húdoková, H., Fleischer, P., Jamnická, G., Kurjak, D., Sliacka Konôpková, A., and Petrík, P.: The combined effect of branch position, temperature, and VPD on gas exchange and water-use efficiency of Norway spruce, Biologia plantarum, 67, 136, 2023.

Reichstein, M., Falge, E., Baldocchi, D., Papale, D., Aubinet, M., Berbigier, P., Bernhofer, C., Buchmann, N., Gilmanov, T., Granier, A., Grünwald, T., Havránková, K., Ilvesniemi, H., Janous, D., Knohl, A., Laurila, T., Lohila, A., Loustau, D., Matteucci, G., Meyers, T., Miglietta, F., Ourcival, J. M., Pumpanen, J., Rambal, S., Rotenberg, E., Sanz, M., Tenhunen, J., Seufert, G., Vaccari, F., Vesala, T., Yakir, D., and Valentini, R.: On the separation of net ecosystem exchange into assimilation and ecosystem respiration:: review and improved algorithm, Global Change Biology, 11, 1424-1439, 10.1111/j.1365-2486.2005.001002.x, 2005.

Ruehr, N. K. and Buchmann, N.: Soil respiration fluxes in a temperate mixed forest: seasonality and temperature sensitivities differ among microbial and root-rhizosphere respiration, Tree Physiology, 30, 165-176, 10.1093/treephys/tpp106, 2010.

Ruehr, N. K., Knohl, A., and Buchmann, N.: Environmental variables controlling soil respiration on diurnal, seasonal and annual time-scales in a mixed mountain forest in Switzerland, Biogeochemistry, 98, 153-170, 10.1007/s10533-009-9383-z, 2010.

Ruehr, N. K., Offermann, C. A., Gessler, A., Winkler, J. B., Ferrio, J. P., Buchmann, N., and Barnard, R. L.: Drought effects on allocation of recent carbon: from beech leaves to soil CO_2 efflux, New Phytologist, 184, 950-961, 10.1111/j.1469-8137.2009.03044.x, 2009.

Rukh, S., Sanders, T. G. M., Krüger, I., Schad, T., and Bolte, A.: Distinct responses of European beech (L.) to drought intensity and length - A review of the impacts of the 2003 and 2018-2019 drought events in central Europe, Forests, 14, 10.3390/f14020248, 2023.

Sabbatini, S., Mammarella, I., Arriga, N., Fratini, G., Graf, A., Hörtriagl, L., Ibrom, A., Longdoz, B., Mauder, M., Merbold, L., Metzger, S., Montagnani, L., Pitacco, A., Rebmann, C., Sedlák, P., Sigut, L., Vitale, D., and Papale, D.: Eddy covariance raw data processing for CO_2 and energy fluxes calculation at ICOS ecosystem stations, International Agrophysics, 32, 495-+, 10.1515/intag-2017-0043, 2018.

Schindlbacher, A., Wunderlich, S., Borken, W., Kitzler, B., Zechmeister-Boltenstern, S., and Jandl, R.: Soil respiration under climate change: prolonged summer drought offsets soil warming effects, Global Change Biology, 18, 2270-2279, 10.1111/j.1365-2486.2012.02696.x, 2012.

Schuldt, B., Buras, A., Arend, M., Vitasse, Y., Beierkuhnlein, C., Damm, A., Gharun, M., Grams, T. E. E., Hauck, M., Hajek, P., Hartmann, H., Hiltbrunner, E., Hoch, G., Holloway-Phillips, M., Körner, C., Larysch, E., Lübbe, T., Nelson, D. B., Rammig, A., Rigling, A., Rose, L., Ruehr, N. K., Schumann, K., Weiser, F., Werner, C., Wohlgemuth, T., Zang, C. S., and Kahmen, A.: A first assessment of the impact of the extreme 2018 summer drought on Central European forests, Basic and Applied Ecology, 45, 86-103, 10.1016/j.baae.2020.04.003, 2020.

Schulze ED, B. E., Buchmann N, Clemens S, Müller-Hohenstein K, Scherer-Lorenzen M Springer (Ed.): Plant Ecology, 2, 928 pp. 2019.

Schwalm, C. R., Williams, C. A., Schaefer, K., Arneth, A., Bonal, D., Buchmann, N., Chen, J. Q., Law, B. E., Lindroth, A., Luyssaert, S., Reichstein, M., and Richardson, A. D.: Assimilation exceeds respiration sensitivity to drought: A FLUXNET synthesis, Global Change Biology, 16, 657-670, 10.1111/j.1365-2486.2009.01991.x, 2010.

Sendall, K. M., Reich, P. B., Zhao, C. M., Hou, J. H., Wei, X. R., Stefanski, A., Rice, K., Rich, R. L., and Montgomery, R. A.: Acclimation of photosynthetic temperature optima of temperate and boreal tree species in response to experimental forest warming, Global Change Biology, 21, 1342-1357, 10.1111/gcb.12781, 2015.

Shapley, L. S.: Stochastic Games, P Natl Acad Sci USA, 39, 1095-1100, DOI 10.1073/pnas.39.10.1095, 1953.

Shekhar, A., Humphrey, V., Buchmann, N., and Gharun, M.: More than three-fold increase of extreme dryness across Europe by end of 21st century, 10.21203/rs.3.rs-3143908/v2, 2023.

Shekhar, A., Chen, J., Bhattacharjee, S., Buras, A., Castro, A. O., Zang, C. S., and Rammig, A.: Capturing the impact of the 2018 European drought and heat across different vegetation types using OCO-2 Solar-Induced Fluorescence, Remote Sensing, 12, 10.3390/rs12193249, 2020.

Shekhar, A., Hörtnagl, L., Paul-Limoges, E., Etzold, S., Zweifel, R., Buchmann, N., and Gharun, M.: Contrasting impact of extreme soil and atmospheric dryness on the functioning of trees and forests, Science of The Total Environment, 10.1016/j.scitotenv.2024.169931, 2024.

Smith, N. G. and Dukes, J. S.: Short-term acclimation to warmer temperatures accelerates leaf carbon exchange processes across plant types, Global Change Biology, 23, 4840-4853, 10.1111/gcb.13735, 2017.

Sperlich, D., Chang, C. T., Peñuelas, J., and Sabaté, S.: Responses of photosynthesis and component processes to drought and temperature stress: are Mediterranean trees fit for climate change?, Tree Physiology, 39, 1783-1805, 10.1093/treephys/tpz089, 2019.

Spinoni, J., Vogt, J. V., Naumann, G., Barbosa, P., and Dosio, A.: Will drought events become more frequent and severe in Europe?, International Journal of Climatology, 38, 1718-1736, 10.1002/joc.5291, 2018.

Strobl, C., Boulesteix, A.-L., Kneib, T., Augustin, T., and Zeileis, A.: Conditional variable importance for random forests, BMC bioinformatics, 9, 1-11, 2008.

Sun, S. Q., Lei, H. Q., and Chang, S. X.: Drought differentially affects autotrophic and heterotrophic soil respiration rates and their temperature sensitivity, Biology and Fertility of Soils, 55, 275-283, 10.1007/s00374-019-01347-w, 2019.

Talmon, Y., Sternberg, M., and Grünzweig, J. M.: Impact of rainfall manipulations and biotic controls on soil respiration in Mediterranean and desert ecosystems along an aridity gradient, Global Change Biology, 17, 1108-1118, 10.1111/j.1365-2486.2010.02285.x, 2011.

Team, R. C.: R: a language and environment for statistical computing. Vienna: R Foundation for Statistical Computing, (No Title), 2021.

Trabucco, A.: Global aridity index and potential evapotranspiration (ET0) climate database v2, CGIAR Consort Spat Inf, 2019.

Tripathy, K. P. and Mishra, A. K.: How Unusual Is the 2022 European Compound Drought and Heatwave Event?, Geophysical Research Letters, 50, 10.1029/2023GL105453, 2023.

van der Molen, M. K., Dolman, A. J., Ciais, P., Eglin, T., Gobron, N., Law, B. E., Meir, P., Peters, W., Phillips, O. L., Reichstein, M., Chen, T., Dekker, S. C., Doubkova, M., Friedl, M. A., Jung, M., van den Hurk, B. J. J. M., de Jeu, R. A. M., Kruijt, B., Ohta, T., Rebel, K. T., Plummer, S., Seneviratne, S. I., Sitch, S., Teuling, A. J., van der Werf, G. R., and Wang, G.: Drought and ecosystem carbon cycling, Agricultural and Forest Meteorology, 151, 765-773, 10.1016/j.agrformet.2011.01.018, 2011.

van der Woude, A. M., Peters, W., Joetzjer, E., Lafont, S., Koren, G., Ciais, P., Ramonet, M., Xu, Y. D., Bastos, A., Botia, S., Sitch, S., de Kok, R., Kneuer, T., Kubistin, D., Jacotot, A., Loubet, B., Herig-Coimbra, P. H., Loustau, D., and Luijkx, I. T.: Temperature extremes of 2022 reduced carbon uptake by forests in Europe, Nature Communications, 14, 10.1038/s41467-023-41851-0, 2023.

van Straaten, O., Veldkamp, E., and Corre, M. D.: Simulated drought reduces soil CO_2 efflux and production in a tropical forest in Sulawesi, Indonesia, Ecosphere, 2, 10.1890/Es11-00079.1, 2011.

von Buttlar, J., Zscheischler, J., Rammig, A., Sippel, S., Reichstein, M., Knohl, A., Jung, M., Menzer, O., Arain, M. A., Buchmann, N., Cescatti, A., Gianelle, D., Kiely, G., Law, B. E., Magliulo, V., Margolis, H., McCaughey, H., Merbold, L., Migliavacca, M., Montagnani, L., Oechel, W., Pavelka, M., Peichl, M., Rambal, S., Raschi, A., Scott, R. L., Vaccari, F. P., van Gorsel, E., Varlagin, A., Wohlfahrt, G., and Mahecha, M. D.: Impacts of droughts and extreme-temperature events on gross primary production and ecosystem respiration: a systematic assessment across ecosystems and climate zones, Biogeosciences, 15, 1293-1318, 10.5194/bg-15-1293-2018, 2018.

Wang, Y. F., Hao, Y. B., Cui, X. Y., Zhao, H. T., Xu, C. Y., Zhou, X. Q., and Xu, Z. H.: Responses of soil respiration and its components to drought stress, Journal of Soils and Sediments, 14, 99-109, 10.1007/s11368-013-0799-7, 2014.

Wang, H., Yan, S. J., Ciais, P., Wigneron, J. P., Liu, L. B., Li, Y., Fu, Z., Ma, H. L., Liang, Z., Wei, F. L., Wang, Y. Y., and Li, S. C.: Exploring complex water stress-gross primary production relationships: Impact of climatic drivers, main effects, and interactive effects, Global Change Biology, 28, 4110-4123, 10.1111/gcb.16201, 2022.

Wang, H., Yan, S. J., Ciaiss, P., Wigneron, J. P., Liu, L. B., Li, Y., Fu, Z., Ma, H. L., Liang, Z., Wei, F. L., Wang, Y. Y., and Li, S. C.: Exploring complex water stress-gross primary production relationships: Impact of climatic drivers, main effects, and interactive effects, Global Change Biology, 28, 4110-4123, 10.1111/gcb.16201, 2022.

Webb, E. K., Pearman, G. I., and Leuning, R.: Correction of Flux Measurements for Density Effects Due to Heat and Water-Vapor Transfer, Quarterly Journal of the Royal Meteorological Society, 106, 85-100, DOI 10.1002/qj.49710644707, 1980.

Xu, B., Arain, M. A., Black, T. A., Law, B. E., Pastorello, G. Z., and Chu, H. S.: Seasonal variability of forest sensitivity to heat and drought stresses: A synthesis based on carbon fluxes from North American forest ecosystems, Global Change Biology, 26, 901-918, 10.1111/gcb.14843, 2020.

Yao, Y., Liu, Y. X., Zhou, S., Song, J. X., and Fu, B. J.: Soil moisture determines the recovery time of ecosystems from drought, Global Change Biology, 29, 3562-3574, 10.1111/gcb.16620, 2023.

Zheng, P. F., Wang, D. D., Yu, X. X., Jia, G. D., Liu, Z. Q., Wang, Y. S., and Zhang, Y. G.: Effects of drought and rainfall events on soil autotrophic respiration and heterotrophic respiration, Agriculture Ecosystems & Environment, 308, 10.1016/j.agee.2020.107267, 2021.

Zhou, S., Williams, A. P., Berg, A. M., Cook, B. I., Zhang, Y., Hagemann, S., Lorenz, R., Seneviratne, S. I., and Gentine, P.: Land-atmosphere feedbacks exacerbate concurrent soil drought and atmospheric aridity, Proceedings of the National Academy of Sciences of the United States of America, 116, 18848-18853, 10.1073/pnas.1904955116, 2019.